sciendo

SOMMERFELTIA 38 (2018)

Sampling bias in presence-only data used for species distribution modelling: theory and methods for detecting sample bias and its effects on models

Bente Støa, Rune Halvorsen, Sabrina Mazzoni and Vladimir I. Gusarov

Rune Halvorsen, Sabrina Mazzoni and Vladimir I. Gusarov, Natural History Museum, University of Oslo, P.O. Box 1172, Blindern, 0318 Oslo, Norway

Bente Støa, Corresponding author. Tel.: +47 90590647, Email address: bente.stoa@nhm.uio.no

Bente Støa, Rune Halvorsen, Sabrina Mazzoni and Vladimir I. Gusarov 2018. Sampling bias in presence-only data used for species distribution modelling: theory and methods for detecting sample bias and its effects on models. – Sommerfeltia 38: 1-53. Oslo. ISBN 978-82-7420-052-7. ISSN 0800-6865. DOI: 10.2478/som-2018-0001.

This paper provides a theoretical understanding of sampling bias in presence-only data in the context of species distribution modelling. This understanding forms the basis for two integrated frameworks, one for detecting sampling bias of different kinds in presence-only data (*the bias assessment framework*) and one for assessing potential effects of sampling bias on species distribution models (*the bias effects framework*). We exemplify the use of these frameworks to museum data for nine insect species in Norway, for which the distribution along the two main bioclimatic gradients (related to oceanicity and temperatures) are modelled using the MaxEnt method. Models of different complexity (achieved by use of two different model selection procedures that represent spatial prediction or ecological response modelling purposes, respectively) were generated with different types of background data (uninformed and background-target-group [BTG]). The bias assessment framework made use of comparisons between observed and theoretical frequency-of-presence (FoP) curves, obtained separately for each combination of species and bioclimatic predictor, to identify potential sampling bias. The bias effects framework made

DOI: 10.2478/som-2018-0001

use of comparisons between modelled response curves (predicted relative FoP curves) and the corresponding observed FoP curves for each combination of species and predictor. The extent to which the observed FoP curves deviated from the expected, smooth and unimodal theoretical FoP curve, varied considerably among the nine insect species. Among-curve differences were, in most cases, interpreted as indications of sampling bias. Using BTG-type background data in many cases introduced strong sampling bias. The predicted relative FoP curves from MaxEnt were, in general, similar to the corresponding observed FoP curves. This indicates that the main structure of the data-sets were adequately summarised by the MaxEnt models (with the options and settings used), in turn suggesting that shortcomings of input data such as sampling bias or omission of important predictors may overshadow the effect of modelling method on the predictive performance of distribution models. The examples indicate that the two proposed frameworks are useful for identification of sampling bias in presence-only data and for choosing settings for distribution modelling options such as the method for extraction of background data points and determining the appropriate level of model complexity.

Keywords: Background target group, frequency of presence, gradient analysis, MaxEnt model complexity, sampling bias, species distribution modelling, species response curves

Contents

INTRODUCTION

Species distribution modelling (SDM, Franklin 2009) comprises methods for integrating geo-referenced observations of presence of a target species with area-covering environmental variables (e.g., Halvorsen 2012). SDM methodology has developed rapidly over the last two decades (Guisan & Zimmermann 2000, Elith et al. 2006, Franklin 2009), but development of this new research field has brought several major challenges of which one is inappropriate use of complex methods available in user-friendly software (Halvorsen 2012, Yackulic et al. 2013). A firm foothold in ecological theory and in-depth understanding of how the methods work is therefore needed (Halvorsen 2012, Merow et al. 2013, Yackulic et al. 2013).

SDM practice involves three main steps (Austin 2007, Halvorsen 2012): (1) collection and preparation of data for the target species and the environmental variables (specification of a data model), (2) parameterization of a statistical model that relates the species' response to the environment (statistical modelling), and (3) model evaluation and assessment. The statistical modelling step does not necessarily make use of geographical co-ordinates; only ecological information for the sites is required. Accordingly, a species distribution model as such is a model of a species' response to potentially important environmental variables, in a conceptual environmental space. Shortcomings in the data or one or more of the statistical modelling steps are likely to reduce model quality by making the modelled response deviate from the 'underlying true response' of the species. The most important potential shortcoming of data used for modeling is that the response variable does not adequately reflect the true response of the species to important environmental variables (Halvorsen 2012).

Natural history museums are one of the most important sources of biodiversity data for distribution modeling although 'museum data' are generally not collected for this purpose. Ideally, sampling for distribution modeling should be random or otherwise designed to represent the entire range of variation along the environmental gradients to which the response is studied. Museum data are, however, likely to be biased towards areas that are easily accessible for biologists, known for their interesting fauna and flora, or that are of special interest for other reasons (Wollan 2008, Robertson et al. 2010, Anderson 2012). Furthermore, museum data are of the presence-only type, not providing explicit information about the environmental conditions under which species are absent. Therefore, distribution models trained with such data may be inaccurate to an extent that is difficult to assess.

Another source of suboptimal distribution models is inadequate model specification and/or sub-optimal model parameterization (Halvorsen 2012). Furthermore, the magnitude of effects of deficiencies and biases in the data, which are likely to be inherited through statistical modelling, may be inflated by the modelling method (Austin 2007).

Good SDM practices require efficient tools and guidelines for assessing bias in the data, for assessing the effects of such bias on modelling results, and for model evaluation (Guisan & Zimmermann 2000, Austin 2007, Halvorsen 2012, Kramer-Schadt et al. 2013). Development of such tools and guidelines requires in-depth understanding of what sampling bias is, and how it affects species distribution models. Most SDM methods in current use are group-discriminative methods (Mateo et al. 2010), by which the ratio of densities of presence observations to all observations (presences and absences) is modelled with respect to variation in supplied environmental variable(s) (Elith et al. 2011, Merow et al. 2013). Because real absence observations are, in cases, unavailable, such data are typically replaced by uninformed background observations, i.e. a set of grid cells from the study area for which no information about eventual presence or absence of the modelled target is available. The uninformed background may consist of all cells of a standard grid superimposed on the study area or a subset of these cells. Use of background

target-group observations (BTG; Phillips & Dudík 2008), typically consisting of presence observations for species that are taxonomically or ecologically related to the modelled target, has been proposed as an alternative to the uninformed background. Appropriateness of BTG for mitigating effects of sampling bias in presence-only data (Phillips & Dudík 2008, Merow et al. 2013, Phillips et al. 2017) rests on the assumptions that the focal species would have been recorded at BTG presence sites if it really occurs there (Phillips & Dudík 2008, Phillips et al. 2009). One further assumption is that the presence and BTG sets of observations contain similar bias (Mateo et al. 2010). The popularity of the BTG approach seems to be rapidly increasing (Graham et al. 2011, Bystriakova et al. 2012, Millar & Blouin-Demers 2012, Crall et al. 2013, Searcy & Shaffer 2014) despite that a thorough evaluation of the approach has not yet been performed (but see Stokland et al. 2011, Heibl & Renner 2012, Fourcade et al. 2014).

Based on gradient analytic (ter Braak & Prentice 1988, Halvorsen 2012) and macroecological (Hengeveld & Haeck 1982, Brown 1984, Cox & Moore 2010) theory, this paper provides two theoretical frameworks, one that addresses identification and categorization of sampling bias in presence-only data (the bias assessment framework) and one for assessing the effects of sampling bias on species distribution models (the bias effects framework). We exemplify use of the frameworks by applying them to data for nine insect species in Norway, the distributions of which are modelled with respect to two important bioclimatic gradients related to oceanicity and temperatures (Moen 1999, Bakkestuen et al. 2008). We apply the frequently used SDM method MaxEnt (Phillips et al. 2006, Phillips & Dudík 2008, Halvorsen 2013, Phillips et al. 2017). The modelling examples are designed to facilitate assessment of the usefulness of the two frameworks and, additionally, to explore the effects of model complexity and use of background target group data on MaxEnt distribution models.

A THEORETICAL UNDERSTANDING OF SAMPLING BIAS IN THE CONTEXT OF SDM

FREQUENCY-OF-PRESENCE (FoP) CURVES: CATEGORIES AND TERMS

A species response curve shows the variation in a species' aggregated performance along an environmental gradient (Halvorsen 2012). The gradient is typically represented by an environmental variable that is recorded (or estimated) for each site in the study area. Response curves are fundamentally important in understanding sampling bias in the SDM context because the response variable, the presence-to-background frequency ratio, is itself a measure of aggregated performance of the species, along the environmental variable (Halvorsen 2012). The obvious choice of aggregated performance measure for presence-only or presence/absence distribution data is the density of the species in a subset of observations units that is homogeneous with respect to the environmental variable in question, e.g., the ratio of the counts of presence and background observations in a subset of observation units with values for the environmental variable within a small interval (Loehle 2012). This measure is referred to in this paper as the Frequency of Presence (FoP). Frequency-of-presence curves (FoP curves) may be obtained as a discrete set of values by counting the number of presence observations in each interval of the gradient (Loehle 2012), or by fitting a continuous response function to densities, e.g., by maximum likelihood estimation methods (Oksanen & Minchin 2002, Jansen & Oksanen 2013).

As a foundation for our theoretical framework, we have defined five types of frequency-of-presence (FoP) curves based on the type of data used to produce them (complete or a subset of an empirical data set, presence-only data combined with selected background data), and absence or presence of bias (see Table 1). The true FoP curve, the empirical FoP curve, the observed FoP curve, the theoretical FoP curve, and the predicted relative FoP curve (the term 'relative' here pertains to the fact that SDMs obtained by use of presence-only data produce output on a relative, not an absolute, probability scale). The first three are all obtained by use of empirical data, differing with respect to the types of presence and background observations used. The true and empirical FoP curves are obtained from presence/absence observations of the target species in the study area, the former requires an exhaustive dataset and assumes full detectability (e.g., MacKenzie et al. 2005), whereas the latter are based upon any sample of presence/absence observations. The observed FoP curves differ fundamentally from the first two by being based on presence-only data and modelled absences (i.e., a set of observations consisting of either uninformed or targeted background observations). In the absence of any kind of bias in the data, the observed FoP is proportionally similar to the true FoP, with a pro-

Table 1. Types of species response curves with definitions.

Term	Definition
True frequency of presence curve	Graph showing the true relative frequency of a species' presence along an environmental gradient, i.e., ratios between counts or densities of presence and background observations for successive intervals or at successive points along the gradient, obtained by use of an exhaustive dataset
Empirical frequency of presence curve	Graph showing variation in the relative frequency of presence observations for a species along an environmental gradient, calculated for successive intervals or at successive points along the gradient as the ratio between counts or densities of presence and absence observations in a relevant but not exhaustive dataset
Observed frequency of presence curve	Graph showing variation in the relative frequency of presence observations for a species along an environmental gradient, calculated for successive intervals or at successive points along the gradient as the ratio between counts or densities of presence and background observations (the background observation set may consist of presences together with uninformed or informed, e.g., background target group, observations)
Theoretical frequency of presence curve	Graph showing variation in the relative frequency of a species along an environmental gradient, deduced from ecological theory and prior knowledge about the species in question
Predicted relative frequency of presence curve	Graph showing variation in the relative predicted frequency (probability) of presence for a species along an environmental gradient, as obtained by an SDM

portionality factor determined by the sampling effort (Loehle 2012).

The theoretical FoP curves show variation in the relative frequency of a species along an environmental gradient under the assumption that no bias of any kind is present. Theoretical FoP curves are deduced from ecological theory and prior knowledge about the species in question. The predicted relative FoP curve is a graphic representation of predictions from a distribution model, i.e., of the results obtained by species distribution modelling.

DEFINITIONS OF SAMPLING BIAS

Sources of bias in presence-only data have been addressed in several studies, and a multitude of terms have been used to categorize such bias, e.g., 'temporal bias' (Bean et al. 2012), 'road-side bias' or 'cosmopolitan bias' (Boakes et al. 2010) and 'hotspot bias' (Loiselle et al. 2008). A clear definition of sampling bias with specific reference to SDM is, however, still lacking [but see Kadmon et al. (2003) and Phillips et al. (2009)].

Bias in response data for SDM can be divided into two types: geographical and environmental sampling bias. We define geographical sampling bias as bias in response data for SDM that occurs because some parts of the geographical space are sampled more intensively than others. Because SDM addresses relationships in the environmental space, i.e., the conceptual space with the major environmental complex-gradients as axes [complex-gradients are sets of environmental gradients that act on species in concert (Whittaker 1967)], geographical sampling bias must manifest itself in the environmental space to affect SDM results. Good performance of group-discriminative SDM methods also requires that the sampling effort be distributed in proportion to the actual frequency distribution of environmental conditions along all environmental variables of importance for the species (Elith et al. 2011). Accordingly, we propose the following operational definition of sampling bias in the context of SDM: A set of presence observations for a target of SDM contains sampling bias if the frequency distribution of observed presences along major environmental complex-gradients deviates from the frequency distribution of the target's true presence in environmental space.

DETECTING SAMPLING BIAS IN PRESENCE-ONLY DATA: THE BIAS ASSESSMENT FRAMEWORK

OUTLINE

Our definition of sampling bias establishes a standard reference for an unbiased sample: the distribution of true frequency of presence of the modelled species in environmental space, i.e., the true FoP curve. A true FoP curve may, if available in a parameterized form, be used as a reference to which the observed FoP curves can be compared by statistical methods or, alternatively, by visual inspection. Deviations of the observed FoP curve from the reference true FoP curve indicate possible presence of sampling bias, as indicated in Fig. 1.

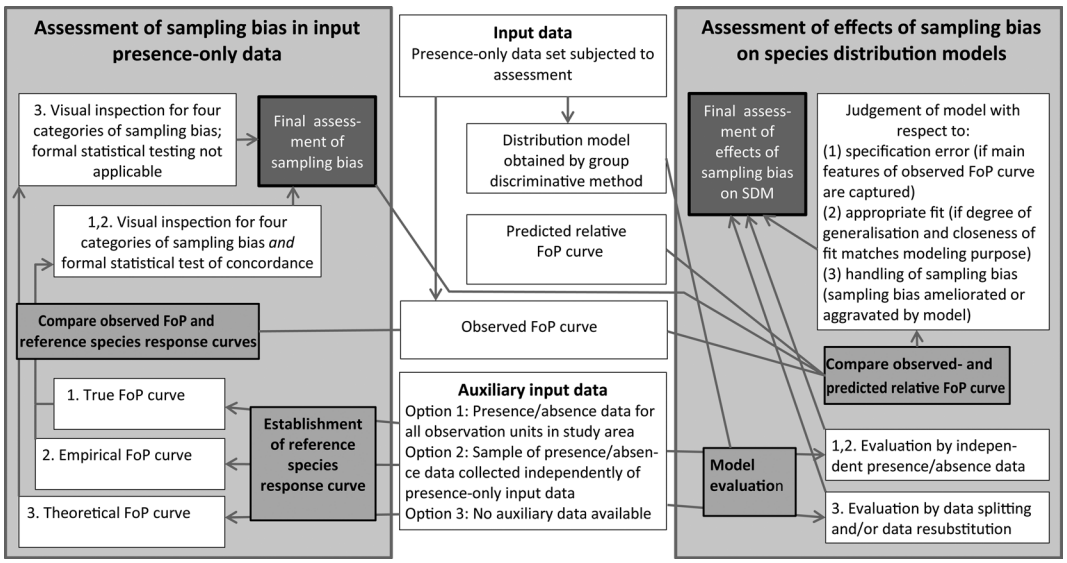

Fig. 1. Proposed frameworks for assessment of sampling bias in presence-only data (left) and for assessment of effects on species distribution models. For explanation, see text.

Unfortunately, obtaining the data required to construct a true FoP curve is unrealistic in almost all cases. In theory, the true FoP curve can be approximated by an empirical FoP curve, constructed by using a sample of high-quality presence/absence data that are collected independently of the data used to obtain the FoP curve (Edvardsen et al. 2011, Erikstad et al. 2013). Fig. 1 shows that empirical FoP curves allow assessment of sampling bias by the same procedures (visual inspection and statistical testing) than theoretical FoP curves.

In most cases, however, also the presence/absence data needed to construct an empirical FoP curve are unavailable, or out of reach given available resources. We are then left with the third alternative shown in Fig. 1: to use the theoretical FoP curves as a reference with which the observed FoP curves can be compared (cf. Vaughan & Ormerod 2003). The theoretical FoP curve is a conceptual rather than a parameterized model, hence the third alternative implies an informal comparison of the observed FoP and the theoretical FoP curves, e.g., by visual inspection, rather than a statistical analysis of relationships. Accordingly, this third option cannot provide conclusive evidence for or against presence of geographical or environmental sampling bias in specific data sets. The value of this option relies on our ability to obtain a reliable theoretical FoP curve. Comparison of observed FoP curves with true, empirical or theoretical, FoP curves forms the basis for the proposed framework for detecting sampling bias in presence-only data intended for use in SDM, as summarised in Fig. 1.

ESTABLISHING THEORETICAL FOP CURVES: GENERAL PROPERTIES OF SPECIES' RESPONSES TO BIOCLIMATIC GRADIENTS

The extent to which comparison of observed FoP curves with theoretical FoP curves will provide valid indications of sampling bias depends on the reliability and realism of the theoretical FoP

curves used in the comparison. We use the gradient analytic perspective (GAP) of Halvorsen (2012), which summarises gradient analytic and macro-ecological biogeographic theory, as a foundation for deriving general properties of theoretical FoP curves. The GAP can be summarised into three points: (1) Species do not respond to single environmental gradients, but to environmental complex-gradients. (2) A few major complex-gradients normally account for most of the variation in species composition that can be explained environmentally, and, most importantly. (3) Species occur within a restricted interval along each major complex-gradient and have an optimum somewhere within this interval. From (3) it follows that theoretical FoP curves should typically be unimodal (Whittaker 1956, Austin & Gaywood 1994), reflecting the preferences for specific parts of the environmental space acquired by each species throughout its evolutionary history. From the species' point of view, habitat suitability and, hence, the species' performance, will decrease with increasing 'environmental distance' from the species' optimum along a complex-gradient. How far away from its optimum a species may be found, depends on the species' physiological tolerance to the resource, stress and/or disturbance factors that vary along the complex-gradient, biotic interactions, and the outcome of demographic processes such as the species' ability to disperse to and establish in new sites (Halvorsen 2012).

The shape of theoretical FoP curves is also influenced by the spatial grain used in the study (sampling-unit size) and by properties of the species and the relevant complex-gradients (Minchin 1989, Økland 1990). Empirical studies ranging from those using small (e.g., 1 m2) plots distributed along local complex-gradients (e.g., Minchin 1989, Rydgren, et al. 2003) to those using larger plots (e.g., 1 km2) distributed along bioclimatic gradients (Brown 1984, Austin & Gaywood 1994) conclude that unimodal responses are typical for species with relatively narrow ecological ranges and optima near the centre of an important complex-gradient. This pattern is found in most species studied (Brown 1984, Halvorsen 2012). Response curves for species with optima near or outside the sampled portion of the complex-gradient will be truncated to various degrees, as shown by Halvorsen (2012: Fig. 11). The unimodal response curve also agrees with conceptual macro-ecological biogeographic models that predict decreasing abundance in geographical space from the centre to the periphery of a species' distributional range, e.g., exemplified by the 'abundant centre model' (Hengeveld & Haeck 1982), the 'peak model for intraspecific patterns' (Gaston et al. 2000, Gaston et al. 2008) and the 'peak-and-tail pattern' (McGill & Collins 2003). Correspondence between a species' response in environmental space and its distribution in geographical space is a logical consequence of the species' geographical distribution reflecting its response to environmental gradients, modified to a greater or lesser extent by its history, biotic interactions and demographic processes.

Available empirical evidence thus supports a generally unimodal shape of theoretical FoP curves with respect to broad-scaled environmental gradients, with exact curve shapes determined by a combination of six factors (see Figs 2–9):

(1) The width of the theoretical FoP curve is determined by the species' tolerance to the environmental conditions that vary along the complex-gradient in question (e.g., Dahl & Birks 1998). The extent to which the response curve will decline gradually or abruptly towards its tails depends on the relationship of the species to the distribution-limiting factors. Species with sharp tolerance limits (Skre 1979, Gauslaa 1984) will have more flat-topped theoretical FoP curves that decline abruptly towards the margins (Fig. 4).

(2) The height of the curve is determined by the local commonness of the species near its optimum (compare Figs 7 and 9).

(3) The width and height of a unimodal theoretical FoP curve tend to be positively correlated. This follows from two important general biogeographic patterns: the positive abundance-occupancy relationship (Brown et al. 1996, Gaston et al. 2000) and the core-satellite species hypothesis (Hanski 1982).

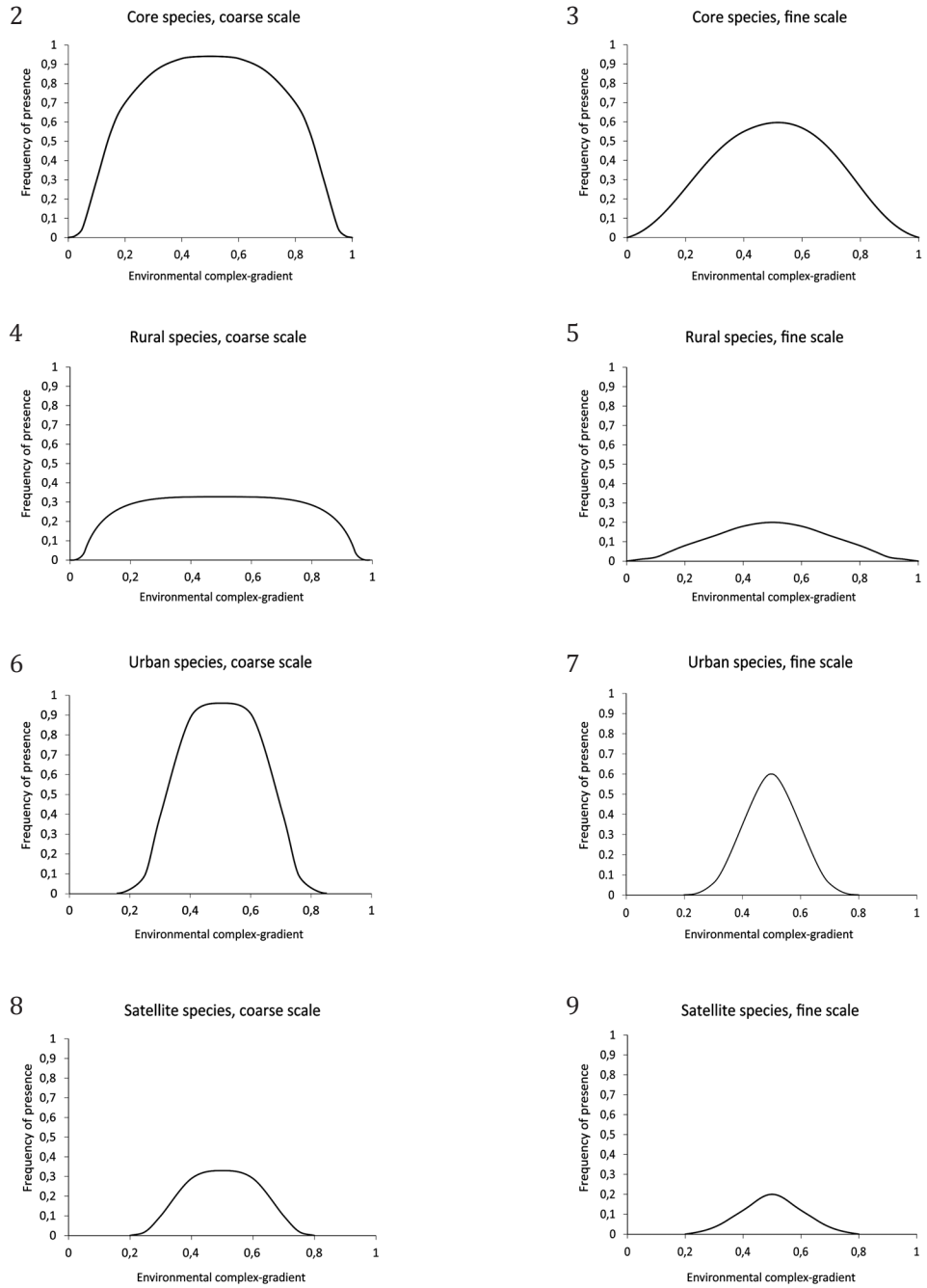

Fig. 2–9. Theoretical frequency-of-presence curves for typical core (2–3), rural (4–5), urban (6–7) and satellite (8–9) species. The species' aggregated performance (given on the ordinate axes) is the relative frequency of a species' presence along the environmental gradient, i.e., ratios between counts or densities of presence and background observations for successive intervals or at successive points along the gradient. Curves are shown for coarse (2, 4, 6, 8) and fine (3, 5, 7, 9) spatial scales, i.e., for coarse (e.g., 100 km2) and fine (e.g., 100 m2) grid-cell rasterizations of the study area, respectively.

(4) The shape of true, empirical, observed and even theoretical FoP curves will be strongly affected by the grain of the study (Loehle 2012): the curves flatten out when grid-cell size increases.

(5) The extent of the study area determines if, or the extent to which, the unimodal theoretical FoP is truncated. Truncation occurs if the full range of the species along the gradient is not contained within the study area (Halvorsen 2012).

(6) The degree of skewness of theoretical FoP curves depends on several factors: (a) If several conditions are met, interspecific biotic interactions may result in skewed empirical responses of species to gradients even when the physiological response [the response in the absence of influence by other species (Ellenberg 1954)] is symmetric (Austin & Smith 1989, Austin & Gaywood 1994, Austin 2002). Because interspecific interactions take place at the spatial scale where individual organisms physically meet (Huston 2002), one such condition is that the interactions manifest themselves at the (typically) much broader scale addressed by SDM. However, the scale at which interspecific interactions take place varies and may be quite broad for larger, more mobile organisms, such as mammals, while it is finer (and normally much finer than the scale addressed in SDM) for smaller, sessile species, such as plants. The larger the study area and the coarser the grid cells used for recording presence or absence, the more individuals have to be involved in interactions to affect the distribution, and hence, the resulting distribution model (Halvorsen 2012). Nevertheless, the SDM literature contains examples of effects of biotic interactions over a wide range of spatial scales. Effects of interspecific interactions on distribution models trained by use of local-scale data have been demonstrated for competition (Meier et al. 2010, Boulangeat et al. 2012), facilitation (Boulangeat et al. 2012), mutualism (Gutiérrez et al. 2005), and parasitic/amensalistic relationships such as effects of the availability of host plants for butterflies (Pellissier et al. 2012). Effects of biotic interactions on regional-scale (1,000–1,000,000 m) distribution models have also been shown, for competition (Leathwick & Austin 2001, Anderson et al. 2002), facilitation (Heikkinen et al. 2007), predation (Hebblewhite et al. 2005), host-plant availability (Araújo & Luoto 2007, Schweiger et al. 2012) and the distribution of prey (Redfern et al. 2006). (b) Irregularities in realized response-curves compared to expectations from theoretical reasoning may be due to metapopulation, or sink-source, dynamics (Hanski & Simberloff 1997, Hanski 1998, Hanski & Ovaskainen 2000). At finer spatial and temporal scales species may occur in unsuitable habitats and be absent from suitable ones because of stochastic processes such as local extinctions and dispersal into temporarily suitable sites (the mass effect; Shmida & Wilson 1985). However, while traditional metapopulation theory assumes that an area consists of discrete patches of suitable habitat surrounded by uniformly unsuitable habitats (but see Cavanaugh et al. 2014), most SDM methods assign a continuous variable value (the relative probability of presence) to each cell in the gridded study area. This improves the realism of model predictions compared to approaches that provide binary predictions. (c) Deviations from a unimodal curve shape by inability of the species to fill its potential range, typically because of interactions between dispersal constraints and available time (Primack & Miao 1992, Hatteland et al. 2013), may result in influences a species' response to one complex-gradient by other complex-gradients with different spatial patterns in the study area (Halvorsen 2012). (d) Local adaptations (Westley et al. 2013). (e) How the gradient is scaled, e.g., in units of physical or chemical units or in units of species compositional turnover (Økland 1986, 1992)

The scale of the study also affects the degree to which each of these possible explanations will influence a distribution model. Dispersal barriers are normally rare when the extent of the study area is small (Soberon & Peterson 2005). At finer scales, biotic interactions and metapopulation dynamics may cause mismatch between the theoretical and the empirical, or observed, FOP curves. Effects of biotic interactions may translate into deviant distributions of

the target species on a broad scale if the interaction is obligate [such as the availability of host plants for host-specific insects (Araújo & Luoto 2007, Schweiger et al. 2012)].

TYPES OF SAMPLING BIAS

We distinguish between four types of sampling bias, each caused by one specific theoretical reason. Sampling biases of types 1–3 are collectively referred to as systematic bias, in contrast to the stochastic variation that constitutes type 4. Each type is characterized by a specific pattern of deviation of the observed FoP curves from the reference true, empirical or theoretical FoP curves. The four types are: (1) under-sampling (Fig. 10), i.e., lower-than-true observed FoP in some intervals along a gradient, (2) over-sampling, i.e., higher-than-true observed FoP in some intervals along a gradient, (3) peripheral sampling gap (Fig. 11), i.e., truncation of the observed FoP curve due to lack of presence observations (in the data set) at one or both of the species' tolerance limits, and (4) stochastic variation (Fig. 12), i.e., irregularities in the observed FoP curve due to unpredictable and variable sampling effort along the gradient.

ASSESSING EFFECTS OF SAMPLING BIAS ON DISTRIBUTION MODELLING RESULTS: THE BIAS EFFECTS FRAMEWORK

The bias effects framework, which provides guidelines for assessing possible effects of sampling bias on the species distribution models as such, is based on comparing the observed FoP curves with the corresponding (modelled response) curves obtained from the modelling results [the predicted relative FoP curve s (Table 1, also see Fig. 1)]. These curves are obtained by using the predicted relative frequencies of presence instead of observed frequencies of presence for calculating aggregated performance.

The ideal SDM method reproduces the true response of the species (i.e., the true FoP curve) with respect to every single environmental variable of importance for the species in an adequate way: (1) if sampling bias is absent, by reproducing the observed FoP curve or, (2) if sampling bias is present, by mitigating any effects of the bias, and (3) by smoothing the response curve to a degree of generality that matches the modelling purpose. This third point highlights that avoidance of overfitting the model to the data is also a means for mitigating sampling bias. In the context of model evaluation, it should be mentioned that evaluation of SDMs has to take modelling purpose into account (Jiménez-Valverde et al. 2008, Halvorsen 2012): spatial prediction modelling and ecological response modelling can be considered as end-points along a gradient of modelling purposes from low to high degrees of generalisation. A (more complex) spatial prediction model is overfit when it reproduces stochastic variation in the training data set, i.e., when the more complex model (in terms of the number of included environmental variables) explains more of the variation in the training data set than a simpler model while the model's prediction error on independently collected data is higher. An ecological response model is overfit when the modelled relationship between the target species and environmental variables cannot be transferred to other areas and/or times without increase of prediction error (Halvorsen 2012). Observed and predicted relative FoP curves with shapes that indicate sampling bias types 1

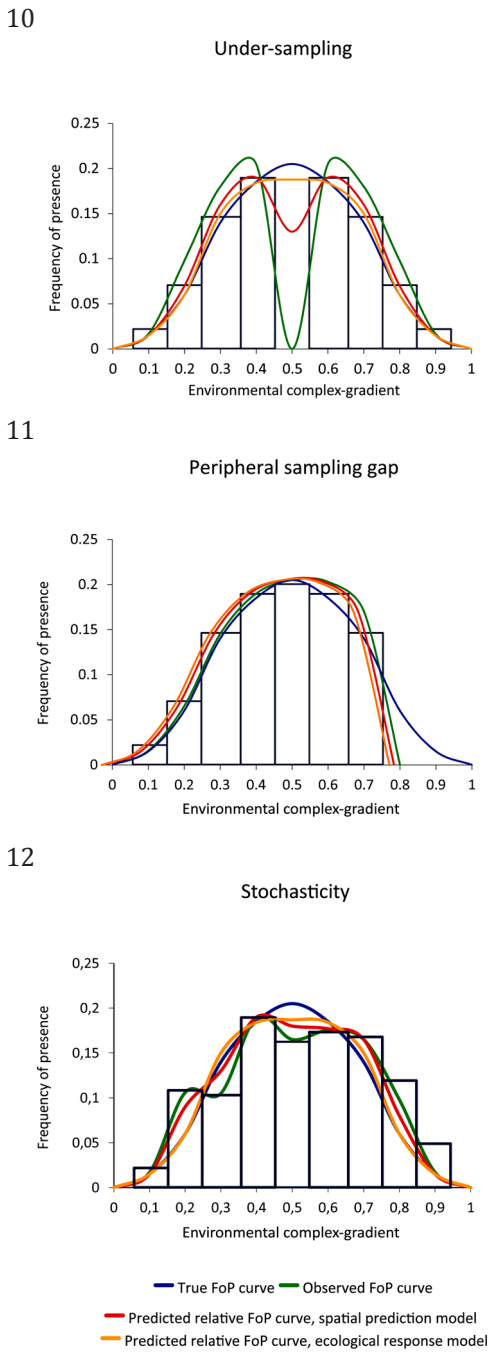

Fig. 10–12. True frequency of presence (FoP) curves, observed frequency of presence curves and predicted relative frequency of presence curves for a hypothetic species, given different types of sampling bias: (10) under-sampling near the species' optimum, (11) peripheral sampling gap, (12) stochastic variation. The bars show the raw frequencies of presence (observed FoP values) which are generalized into the observed FoP curve.

and 2 (gaps and over-sampling) may, however, also result from real properties of the modelled species in a study area, resulting, e.g., from biotic interactions or inability of the species to fill its ecological range. These curve shapes are thus compatible with valid spatial prediction models while they are inappropriate in ecological response modelling contexts because they do not represent general properties of the species. If the purpose is ecological response modelling, such patterns indicate a need for stronger smoothing of the model. Sampling bias type 3, peripheral sampling gaps (Fig. 12), will affect the skewness of observed FoP (and predicted relative FoP) curves and can normally not be identified without access to auxiliary presence/absence data. Sampling bias type 4 (stochastic variation) can be confidently identified and interpreted as an indication of sampling bias by inspecting observed and predicted relative FoP curves . This is also the only type of sampling bias that may be mitigated by a modelling method without introducing new bias to the model. We therefore argue that, unless there are strong indications for the opposite, SDM methods should produce predicted relative FoP curves that reproduce observed FoP curves as closely as possible and with a degree of detail that matches the level of generalization required by the purpose of the study (Halvorsen 2012). Furthermore, we argue that datasets that give rise to observed FoP curves that appear unrealistic because of sampling bias should be rejected or improved before they are subjected to SDM.

Besides assessment of sampling bias effects, comparisons between observed FoP and predicted relative FoP curves may reveal modelling bias, i.e., shortcomings of the model as such. The most important type of modelling bias is model specification errors, whereby the model does not capture important features of observed FoP-curve shapes. Comparisons between observed and predicted relative FoP curves do, however, not provide an alternative to model evaluation by standard tools for assessing the model's predictive ability (from a spatial predictive modelling perspective), which are needed, among others, for selection among alternative models (Halvorsen 2012). Evaluation of SDM models, if possible, should be performed by use of independently collected presence/absence datasets (Phillips & Elith 2010, Edvardsen et al. 2011, Halvorsen 2012, Erikstad et al. 2013). Such datasets can also be used to provide true FoP curves that are useful for identifying and assessing sampling bias (cf. Fig. 1).

EXAMPLES: THE TWO FRAMEWORKS APPLIED TO DATA FOR NINE INSECT SPECIES IN NORWAY

STUDY AREA

We exemplify use of the bias assessment and bias effects frameworks by applying them to data and distribution modelling results for nine insect species in Norway (Table 2). Our study area is the mainland of Norway, which comprises 323,782 km2. Norway is particularly well suited for exploring SDM-related issues because of the two strong bioclimatic gradients: one related to oceanicity-continentality and the division into bioclimatic sections (from strongly oceanic to slightly continental), and the other related to temperature and the division into bioclimatic zones (boreo-nemoral to the high alpine; Moen 1999, Wollan et al. 2008). Large topographical and geological diversity, and complex spatial and temporal variation in human land-use, makes the study area highly variable with respect to environmental conditions and species composition (Halvorsen 2012).

Table 2. Properties of the nine species used for the examples: numbers of presence observations and distribution in Norway. CURS category refers to the classification by Collins et al. (1993) of species according to the spatial abundance and distribution pattern as core, urban, rural or satellite (the hierarchical continuum model). The 'intermediate' category denotes a species that did not fit into any of the four categories. BTG = Background target group.

Species	Family (BTG)	Order	No. of presence observations	No. of BTG presence observations	Distribution in Norway	CURS category	Trophic level	Red List Status
Meligethes aeneus	Nitidulidae	Coleoptera	60	443	north to Troms county	Intermediate	Herbivore	–
Dioctria hyalipennis	Asilidae	Diptera	95	375	S. Norway, with concen tration to southeast Norway	Intermediate	Predator	–
Glaucopsyche alexis	Lycaenidae	Lepidoptera	84	1541	SE Norway along the coast	Satellite	Herbivore	NT
Rhagium mordax	Cerambycidae	Coleoptera	111	1228	the whole country except the high north	Core	Herbivore	–
Volucella bombylans	Syrphidae	Diptera	103	598	the whole country below the tree line	Core	Adults herbivore, larvae scavenger	–
Parnassius apollo	Papilionidae	Lepidoptera	88	211	inland SE Norway	Urban	Herbivore	–
Rhagonycha limbata	Cantharidae	Coleoptera	113	312	the whole country below the tree line	Core	Predator	–
Eristalis intricaria	Syrphidae	Diptera	194	598	the whole country below the tree line	Core	Adults herbivore, larvae detrivore	–
Pieris napi	Pieridae	Lepidoptera	346	926	the whole country	Core	Herbivore	–

MATERIAL: SPECIES PRESENCE DATASETS

Species occurrence data for nine species from three insect orders were used for the examples (Table 2). The species were assigned to the four CURS categories (plus one indeterminate, or intermediate, category, for species that did not fit into one of these four categories) of the hierarchical continuum model of Collins et al. (1993) by their abundance and distribution patterns (Figs 2–9): core (C) species with high maximum abundance and wide tolerance (to the gradients(s) in question) and hence broad distribution; urban species with high abundance and narrow distribution; rural species which combine low maximum abundance with broad distribution, and satellite species with low abundance and narrow distribution. Classification of the species to CURS category was done by visual comparison of the shape of empirical FoP curves provided by earlier studies (Hansen & Larsson 1973, Ehnström & Holmer 2007, Aarvik et al. 2009, Bartsch et al. 2009) with the theoretical FoP curves in Figs 2–9.

Presence observations for the nine focal species and other species belonging to the same family (cf. Table 2) were extracted from the databases of the insect collections of three Norwegian institutions: the Natural History Museum, University of Oslo; Bergen Museum, University of Bergen; and the Museum of Natural History and Archaeology, Norwegian University of Science and Technology, Trondheim. Only records that could be geo-referenced with precision ± 1000 m or better were included.

Accepted presence records were assigned to cells in a 1 × 1 km grid covering the study area. Multiple records within the same grid cell were treated as one observation. Since no information about bioclimatic gradient positions (see below) was available for grid cells with the centre point falling in the sea, the few presence records in such grid cells were assigned to the nearest grid cell for which bioclimatic gradient information was available.

MATERIAL: EXPLANATORY VARIABLES

As explanatory variables we used two variables that represent the two most important regional bioclimatic gradients in Norway (Bakkestuen et al. 2008, Moen 1999): the oceanicity-continentality gradient (Figs 13, 15) and the temperature gradient (Figs 14, 16). The two continuous variables were obtained for 1 × 1 km cells covering the study area according to Bakkestuen et al. (2008) , i.e., as the two directions in the space spanned by the first two axes of a PCA ordination of 54 climatic, topographical, hydrological and geological variables of that best corresponded with the divisions into vegetation sections and vegetation zones described by Moen (1999). The two variables were transformed from the original scaling in arbitrary units onto a 0–1 scale. The fact that PCA axes 1 and 2 together accounted for 63 % of the variation in the set of 54 variables subjected to ordination by Bakkestuen et al. (2008) shows that the oceanicity-continentality and temperature gradients, and the variables we used to represent them, can validly be used as continuous representations of the discrete vegetation sections and zones.

METHODS: DISTRIBUTION MODELLING BY MAXENT

Distribution models were developed using Maxent software, version 3.3.3k (Phillips et al. 2006), which apply the MaxEnt method (the software is referred to as Maxent and the modelling method

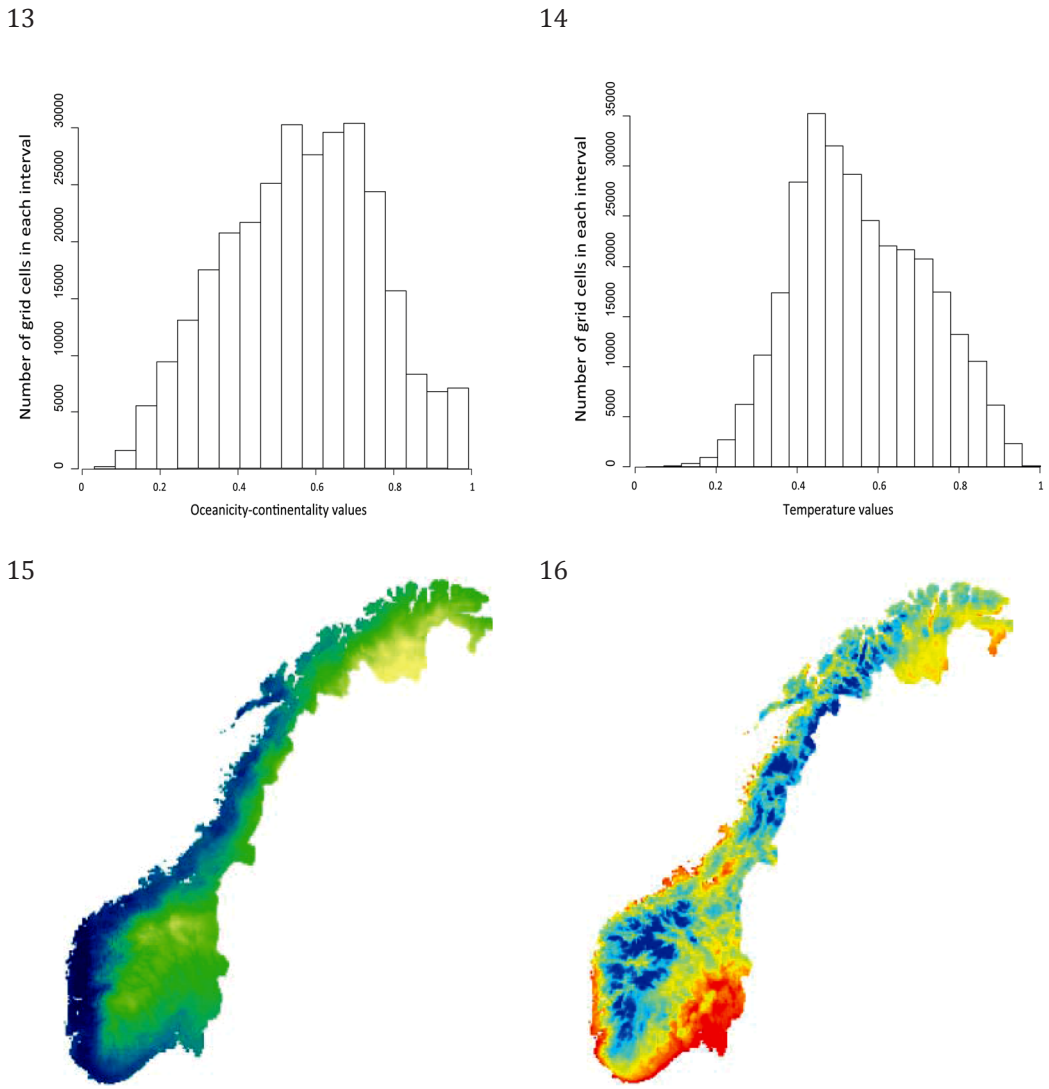

Fig. 13–16. Variation along the continuous oceanicity-continentality (13, 15) and temperature (14, 16) gradients (both scaled from zero to 1) over mainland Norway: frequency distributions of grid cells along each gradient (13, 14) and geographical distributions of gradient values (15, 16). The oceanicity-continentality gradient runs from oceanic (blue, low values) to slightly continental (yellow) while the temperature gradient runs from arctic-alpine (blue, low values) to temperate (boreo-nemoral; red).

as MaxEnt). MaxEnt, which is based on the maximum entropy principle (Jaynes 1957a, 1957b), has been described alternatively as a machine-learning method (Phillips et al. 2006, Phillips & Dudík 2008, Elith et al. 2011), as a method that is based on principles of Bayesian estimation (Elith et al. 2011, Merow et al. 2013), and as a maximum likelihood estimation method (Halvorsen 2013, Renner & Warton 2013, Halvorsen et al. 2014). MaxEnt estimates the relative probability distribution of maximum entropy for the modelled target (Phillips et al. 2004).

Spatial prediction models were obtained by the so-called default MaxEnt practice, i.e., by use of the default Maxent program settings for all options (see Phillips & Dudík 2008, Halvorsen et al. 2015) except one: the raw output format was used instead of the default, logistic, format in accordance with recommendations by Halvorsen (2013) and Yackulic et al. (2013). The default MaxEnt procedure implies: (1) that derived variables of up to five types (linear, quadratic, hinge, threshold and product) were obtained by the 'autofeatures' procedure for each combination of explanatory variable and species (*M. aeneus* excepted, this species had too low frequency for threshold and product variables to be generated), and (2) variable selection by ℓ_1-regularisation (Hastie et al. 2009), also described as the lasso penalty (Tibshirani 1996), which is a parameter shrinkage model selection method (Reineking & Schröder 2006, Halvorsen 2013, Merow et al. 2013) by which the strictness of the variable selection criterion is determined by a regularization multiplier (the default parameter value of 1 was used). The number of derived variables selected for each model was read from the Maxent output file NN.lambdas as the number of nonzero model parameters (Warren and Seifert 2011).

Ecological response MaxEnt models were obtained by the forward stepwise variable selection procedure described by Halvorsen (2013) and Halvorsen et al. (2015). This subset selection method (Reineking & Schröder 2006) proceeds in two phases, each consisting of an iteration process that makes use of a model optimization criterion based upon comparison of variations accounted for by nested MaxEnt models (Halvorsen 2013). In phase (1) a parsimonious set of derived variables was selected to represent each explanatory variable, in phase (2) a parsimonious set of explanatory variables, each represented by the set of derived variables resulting from step (1), was selected. The model optimization criterion used was that the more complex model should improve the simpler model more than expected of a random model of comparable complexity, as judged by an F-ratio test with significance level $\alpha = 1 \bullet 10-6$. All five types of derived variables that were considered for spatial prediction models, except product (interaction) variables, were considered. In addition, a sixth derived variable type, the deviation variable, was obtained for all combinations of species and explanatory variables for which the FOP curve (after smoothing) had a distinct peak. The deviation variable is the set of absolute value differences between the estimated optimum and explanatory variable values, calculated for each grid cell.

Ecological response models were parameterized by use of customized R scripts (Halvorsen et al. 2015, Mazzoni et al. 2015), wrapped around the Maxent software (Phillips et al. 2006, Phillips & Dudík 2008), now available in the MIAmaxent R package (Vollering et al. 2016). For each of the nine species, spatial prediction and environmental response MaxEnt models were obtained separately for two sets of background observations: (1) uninformed background (UB), which consisted of the respective presence observations and 10,000 randomly selected grid cells for which nothing was known about presence or absence; and (2) background target group (BTG) background, which consisted of all georeferenced presence observations in the database of the insect collection of the Natural History Museum, University of Oslo, for all species that belonged to the same family as the respective focal species, the focal species included (Table 2).

The raw model output values were transformed into PRO (probability-ratio output) values (Halvorsen 2013, Halvorsen et al. 2015) by multiplication of each raw output value by the total number of background observations. Probability-ratio output differs from raw output by being independent of the number of background observations and by having a mean value of 1.

METHODS: COMPARISON BETWEEN MAXENT MODELS

We used the area under the receiver operating curve (AUC), adjusted for use with presence-only data (transformed AUC, tAUC) in accordance with Halvorsen (2013), as a measure of model performance:

$$tAUC = (AUC - \phi/2)/(1 - \phi) \ ,$$

where ϕ is the number of presence observations divided by the number of background observations. Transformed AUC values are recorded on the full 0–1 scale, and are thus comparable with (untransformed) AUC values for presence/absence data. tAUC values of 0.5 and 1.0 correspond to models that are random, and that perfectly discriminate between presences and (pseudo-) absences, respectively, AUC expresses variation in the fractions of correctly predicted presences and correctly predicted (pseudo-)absences over the entire range of threshold values for relative predicted probability of presence (Pearce & Ferrier 2000). AUC values above 0.9 are commonly considered to indicate 'very good' predictive performance (Araújo & Guisan 2006).

The two model properties, tAUC and the number of derived variables, were tested for differences among model selection methods, background datasets and species, by generalized linear models (GLM; Crawley 2013). Identity link and normal errors and log link and Poisson-distributed errors were used for the two response variables, respectively.

METHODS: APPLYING THE BIAS ASSESSMENT AND THE BIAS EFFECTS FRAMEWORKS

Presence of sampling bias in the datasets was evaluated by using the procedure outlined in the bias assessment framework (Fig. 1). Hence, the observed FoP curves for each species along the oceanicity-continentality and the temperature gradients, respectively, were compared with theoretical FoP curves for each combination of species and gradient, obtained by first choosing the appropriate template from Figs 2–9 and adjusting it by use of information about species ranges and abundances in Table 2.

The FoP curves were made by the method proposed by Loehle (2012): each explanatory variable was first divided into 20 quantiles (each comprising 5% of all grid cells in the study area) and for each quantile, the ratio of number-of-presence to number-of-background observations was calculated. FoP curves were obtained by plotting observed FoP against the quantile midpoints. In order to improve the visualization of the observed FoP curves, we applied a three-point moving average smoothing procedure three consecutive times to the raw observed FoP values (with weights of 1, 2 and 1 for the three consecutive quantile classes).

Effects of sampling bias on MaxEnt models were evaluated by using the bias effects framework. We first obtained predicted relative FoP curves from MaxEnt modelling results, using the modelled relative predicted probabilities of presence (RPPP values, in PRO format) instead of observed presences for calculating aggregated performance values. In total, 72 predicted relative FoP curves were obtained [9 species × 2 MaxEnt modelling setups × 2 sets of background observations × 2 explanatory variables] by averaging model output predictions for each of the 20 quantiles into which each explanatory variable was divided. Thereafter we compared the predicted relative FoP curves with the corresponding observed FoP and theoretical FoP curves.

RESULTS: IDENTIFICATION OF SAMPLING BIAS

The observed FoP curves along the oceanicity-continentality gradient, using uninformed background (Fig. 17–52), fell into two groups. The first group consisted of the five core species (Table 2) for which observed FoP curves varied considerably: *R. mordax* had a uni- to bimodal curve (Fig. 17), *P. napi* had an irregular, bi- to trimodal curve (Fig. 49), whereas *V. bombylans* (Fig. 33), *R. limbata* (Fig. 41) and *E. intricaria* (Fig. 45) had more or less irregular curves that decreased towards the continental end of the gradient. The second group, which consisted of the intermediate, urban and satellite species (Table 2), had distinctly unimodal observed FoP curves: For *G. alexis*, an almost smooth observed FoP curve was obtained (Fig. 25), whereas the observed FoP curves for *P. apollo* (Fig. 37), *D. hyalipennis* (Fig. 21) and *M. aeneus* (Fig. 17) were somewhat irregular, with sharper peaks than expected (compare with Figs 2–9).

All observed FoP curves along the temperature gradient, using uninformed background (Figs 19, 23, 27, 31, 35, 39, 43, 47 and 51), increased more or less monotonously towards the high-temperature gradient end and only minor irregularities were observed, even before smoothing.

Observed FoP curves along the oceanicity-continentality gradient, using the BTG background, varied in an unique way for the five core species (Fig. 30, 34, 42, 46 and 50), whereas unimodal curve shapes were obtained, even after smoothing, for the satellite (Fig. 26) and intermediate species (Fig. 18 and 22). A bimodal curve was obtained for *P. apollo*, the only urban species (Fig. 38).

The tendency for the observed FoP curves based on uninformed background data to increase towards high temperatures was weakened for all the nine species when BTG was used (Fig. 20, 24, 28, 32, 36, 40, 44, 48 and 52). [Note that the vertical axes of corresponding uninformed background- and BTG-based curves (see Figs 17–52) have different scales. The curves are therefore comparable only with respect to shape and not with respect to amplitude along the vertical axis.] Concerning the temperature gradient, all observed FoP curves calculated with BTG were more irregular than the corresponding curves based on uninformed background. Four species had observed FoP–BTG curves that differed considerably from the corresponding uninformed background curves: the satellite species, *G. alexis* (Figs 27 and 28), the core species, *R. mordax* (Figs 31 and 32) and *R. limbata* (Figs 43 and 44), and the urban species, *P. apollo* (Figs 39 and 40).

Fig. 17–52. Observed frequency of presence (FoP) curves for combinations of explanatory variable (the oceanicity-continentality and temperature gradients), type of background data used [uninformed background and background target group (BTG), which together with presence observations make up the background], and species. Explanatory variables were divided into 20 quantile classes. Black lines show observed FoP curves, calculated for each quantile class as the number of presences divided by the number of background observations. Red, dashed lines show smoothed observed FoP curves. The grey areas in observed FoP curves for BTG background show intervals along the horizontal axis that are devoid of BTG observations.

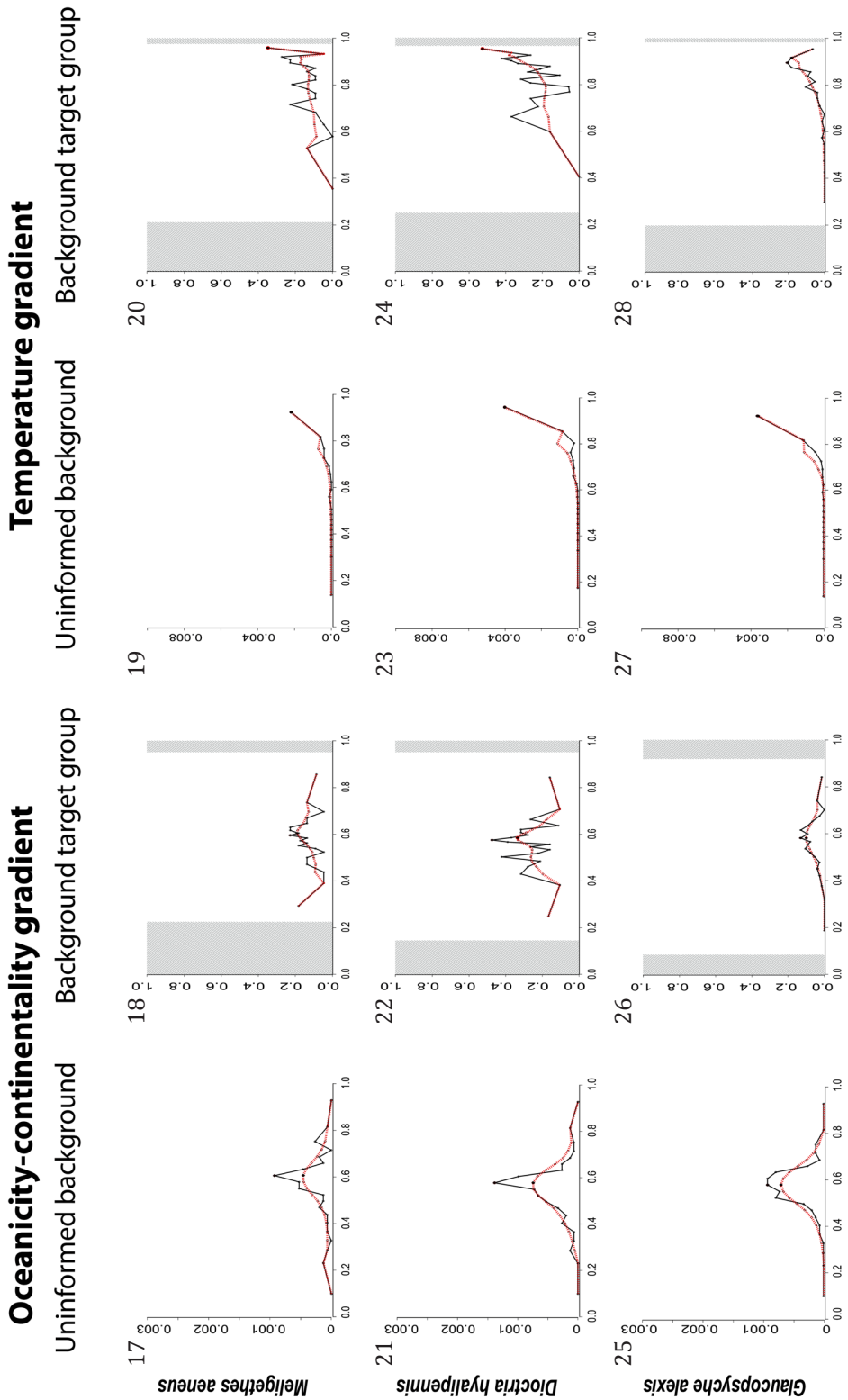
Oceanicity-continentality gradient
Temperature gradient
Uninformed background
Background target group
Uninformed background
Background target group
Melligethes aeneus
Diictria hyalipennis
Glaucopsyche alexis
17
18
19
20
21
22
23
24
25
26
27
28

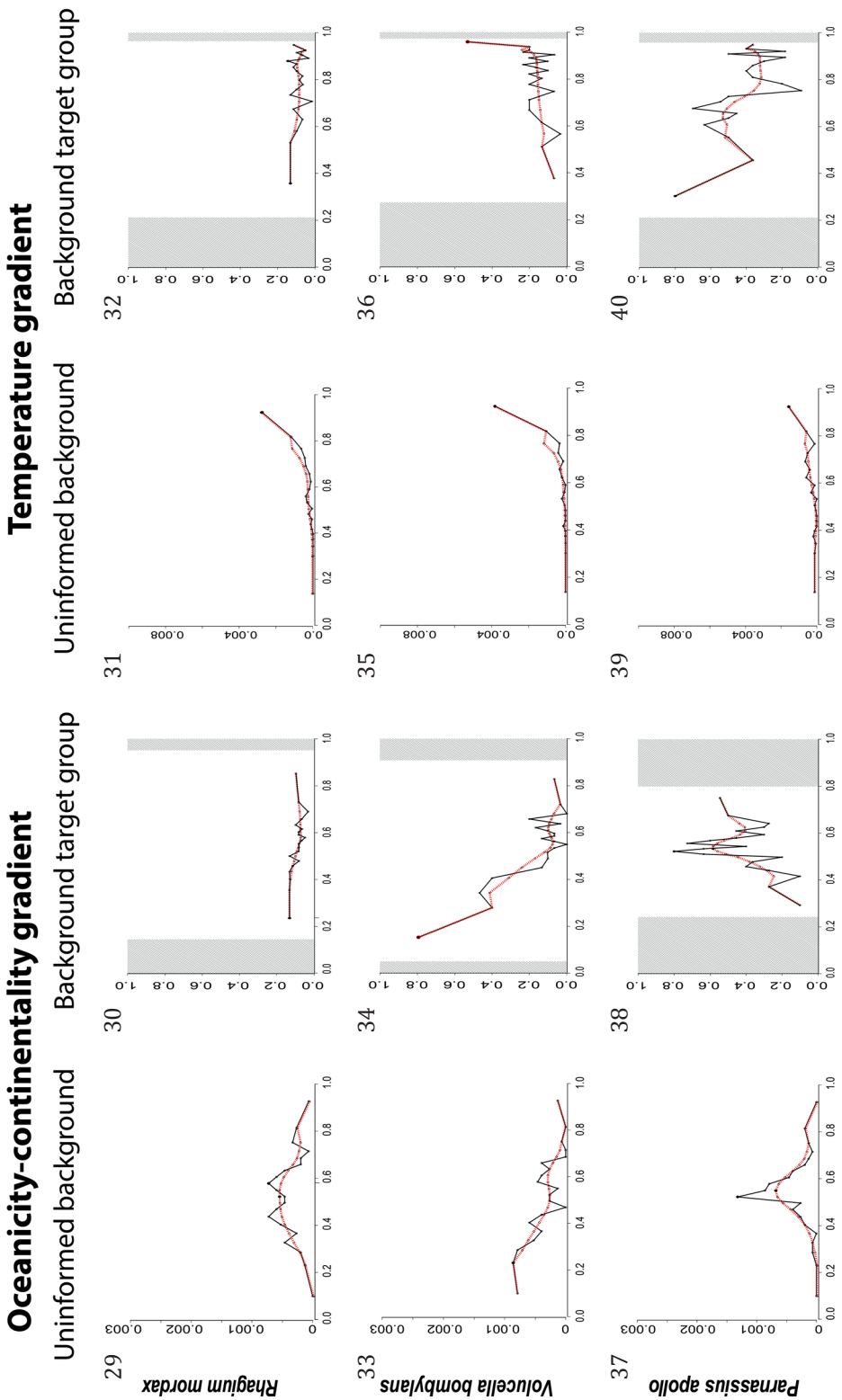
Oceanicity-continentality gradient
Temperature gradient
Uninformed background
Background target group
Uninformed background
Background target group
Rhagium mordax
Volucella bombylans
Parnassius apollo
29
30
31
32
33
34
35
36
37
38
39
40

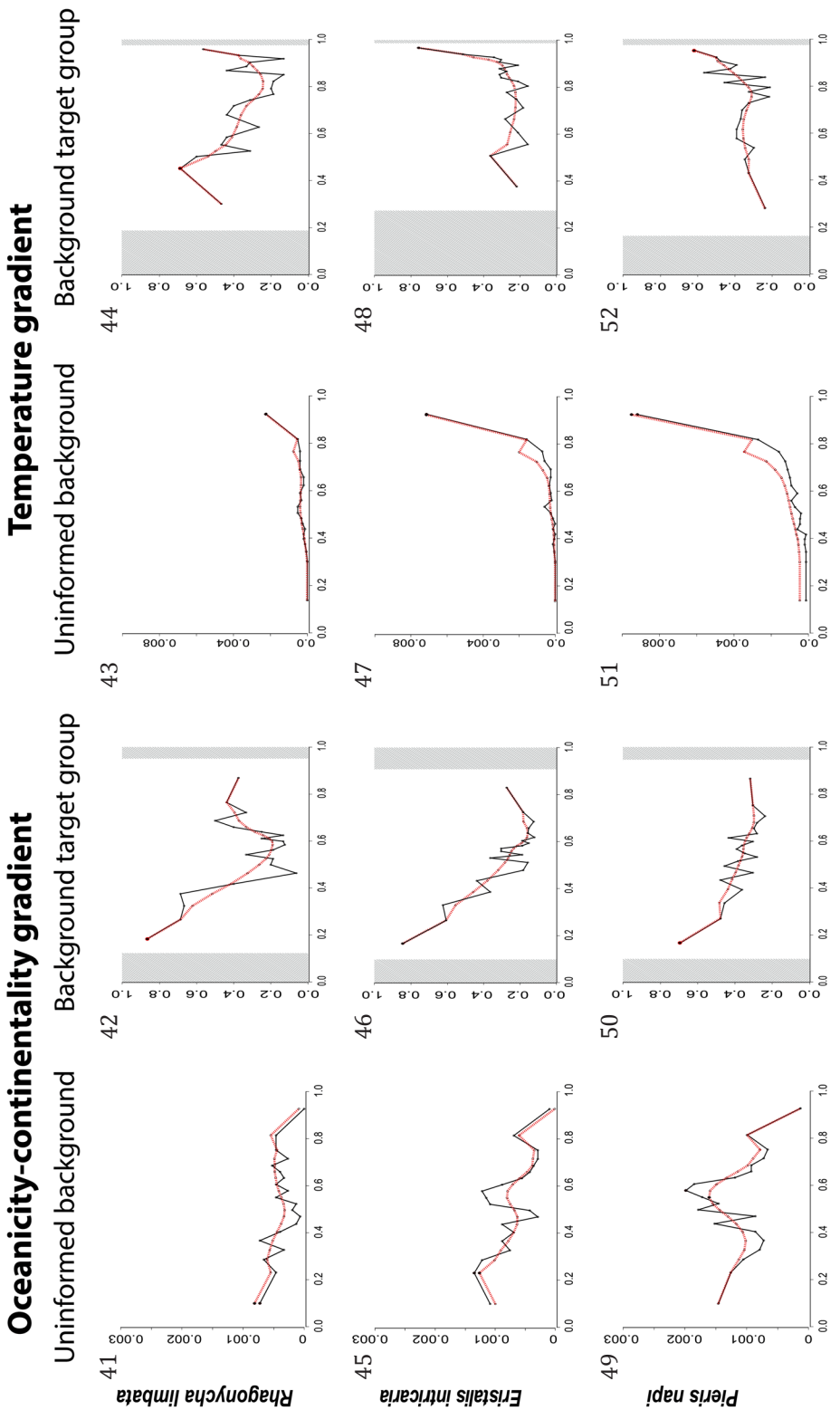
Oceanicity-continentality gradient
Temperature gradient
Uninformed background
Background target group
Uninformed background
Background target group
Rhagonycha limbata
Eristalis intricaria
Pieris napi
41
42
43
44
45
46
47
48
49
50
51
52

RESULTS: ASSESSMENT OF EFFECTS OF SAMPLING BIAS

The predicted relative FoP curves with respect to the oceanicity-continentality gradient, using uninformed background (Fig. 53–88), were relatively smooth, and for the most similar within the ecological response models and the spatial prediction models (i.e. applying the two different model selection approaches), and with only small differences from the corresponding observed FoP curves.

Predicted relative FoP curves obtained using BTG differed more strongly from the observed FoP curves than curves obtained using uninformed background data (compare Figs 17–52 with corresponding Figs 53–88). Of the three species with unimodal observed FoP–BTG curves along the oceanicity-continentality gradient, only one, the satellite species, *G. alexis*, had a distinctly unimodal predicted relative FoP curve (Fig. 62). For the other two species, *M. aeneus* (Fig. 54) and *D. hyalipennis* (Fig. 58), the predicted relative FoP-BTG curve for the ecological response model showed no distinct trend along the oceanicity-continentality gradient whereas the spatial prediction model predicted a complex, unimodal relationship. For the remaining six species, predicted relative FoP–BTG curves were more or less similar to the observed FoP curves (Figs 66, 70, 74, 78, 82 and 86).

For all combinations of species, MaxEnt model (spatial prediction model or ecological response model), and type of background data, the observed FoP and the predicted relative FoP curves along the temperature gradient had similar shapes (compare Figs 17–52 with corresponding Figs 53–88).

Ecological response models in which one explanatory variable was represented by few or no derived variables (Table 3) gave rise to predicted relative FoP curves without clear patterns. This was evident in the ecological response models with BTG background for *D. hyalipennis* along the oceanicity-continentality gradient (Fig. 58) and for *V. bombylans* along the temperature gradient (Fig. 72). Predicted relative FoP curves with piecewise flattened or linear segments resulted from models with derived variables of the threshold and/or hinge types (Appendix 1–4, Fig. 60, 66, 68, 70 and 74). Maps of the geographical distribution of probability-ratio output values from all models are shown in Figs 89–124.

Fig. 53–88. Predicted relative frequency of presence curves for combinations of explanatory variable (the oceanicity-continentality and temperature gradients), type of background data used [uninformed background and background target group (BTG), which together with presence observations make up the background], and species. Black lines and predictions show predictions from ecological response models from spatial prediction models by red, dashed lines. Explanatory variables were divided into 20 quantile classes. Average predicted relative FoP, calculated for each quantile class, is shown on the vertical axes. The grey areas in predicted relative FoP curves for BTG background show intervals along the horizontal axis that are devoid of BTG observations. Each grey dot represents one predicted value from the ecological response model.

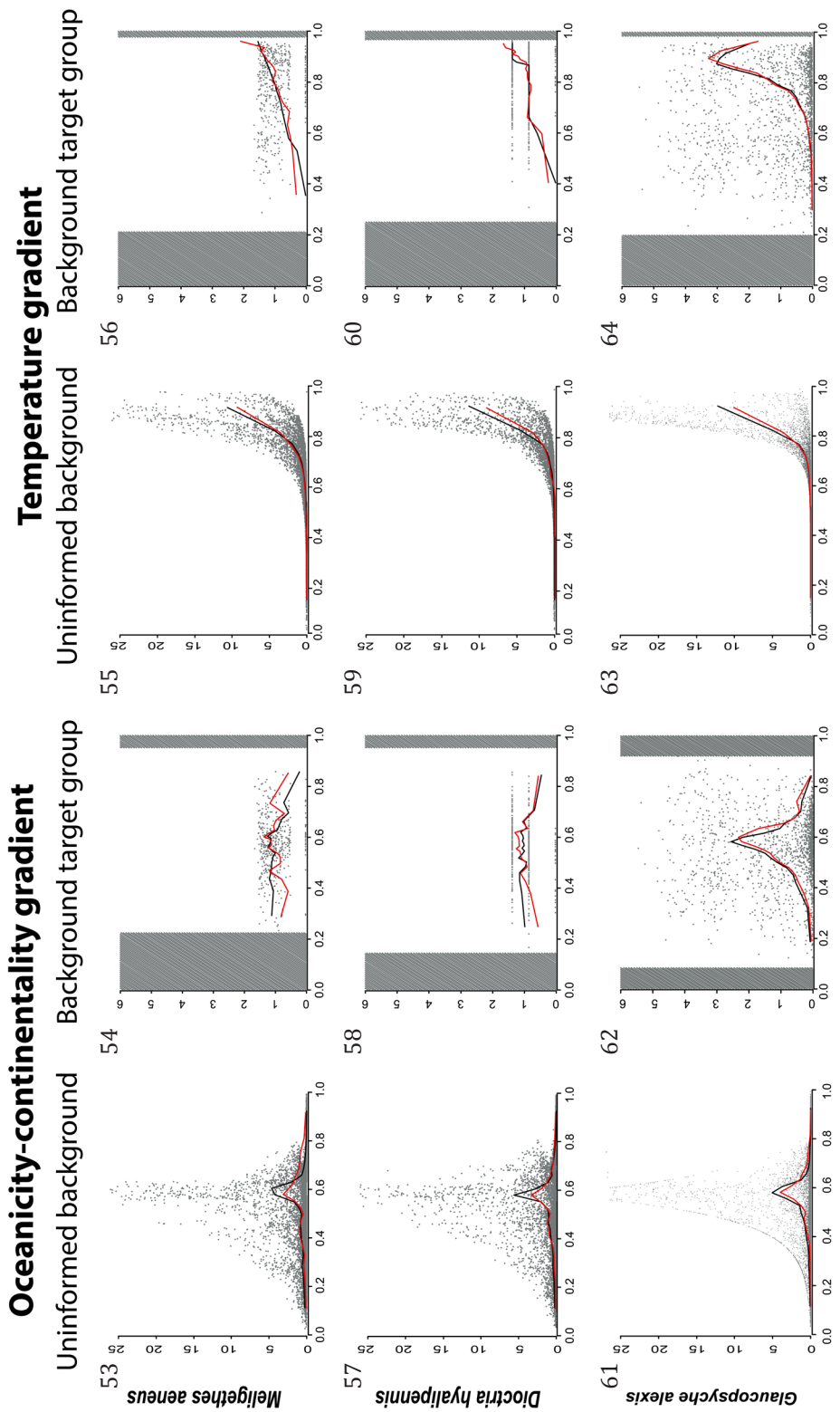
Oceanicity-continentality gradient
Uninformed background
Background target group
Temperature gradient
Uninformed background
Background target group
Melligethes aeneus
Diictria hyallipennis
Glaucopsyche alexis
53
54
55
56
57
58
59
60
61
62
63
64

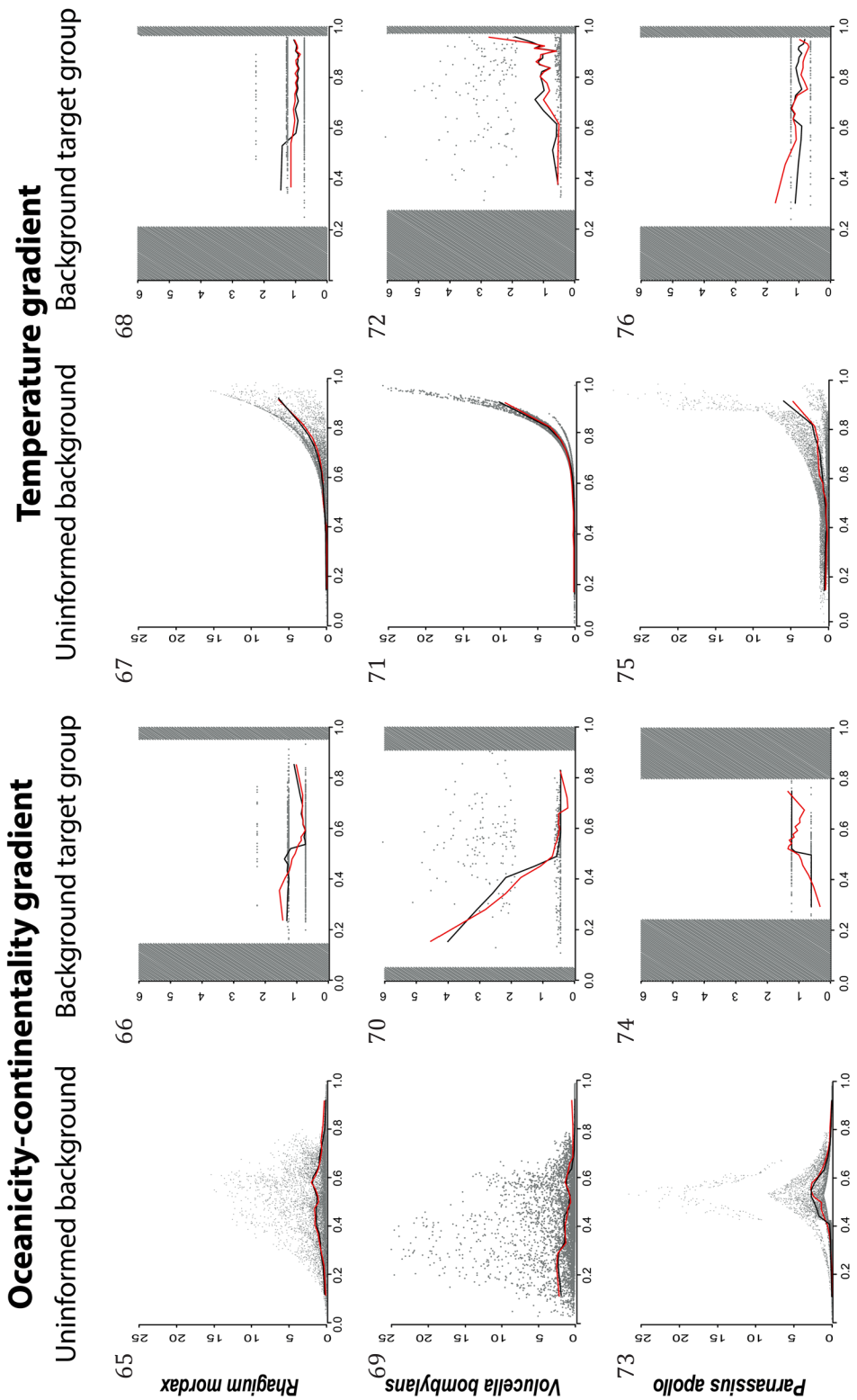
Oceanicity-continentality gradient
Uninformed background
Background target group
Temperature gradient
Uninformed background
Background target group
Rhagium mordax
Volucella bombylans
Parnassius apollo
65
66
67
68
69
70
71
72
73
74
75
76

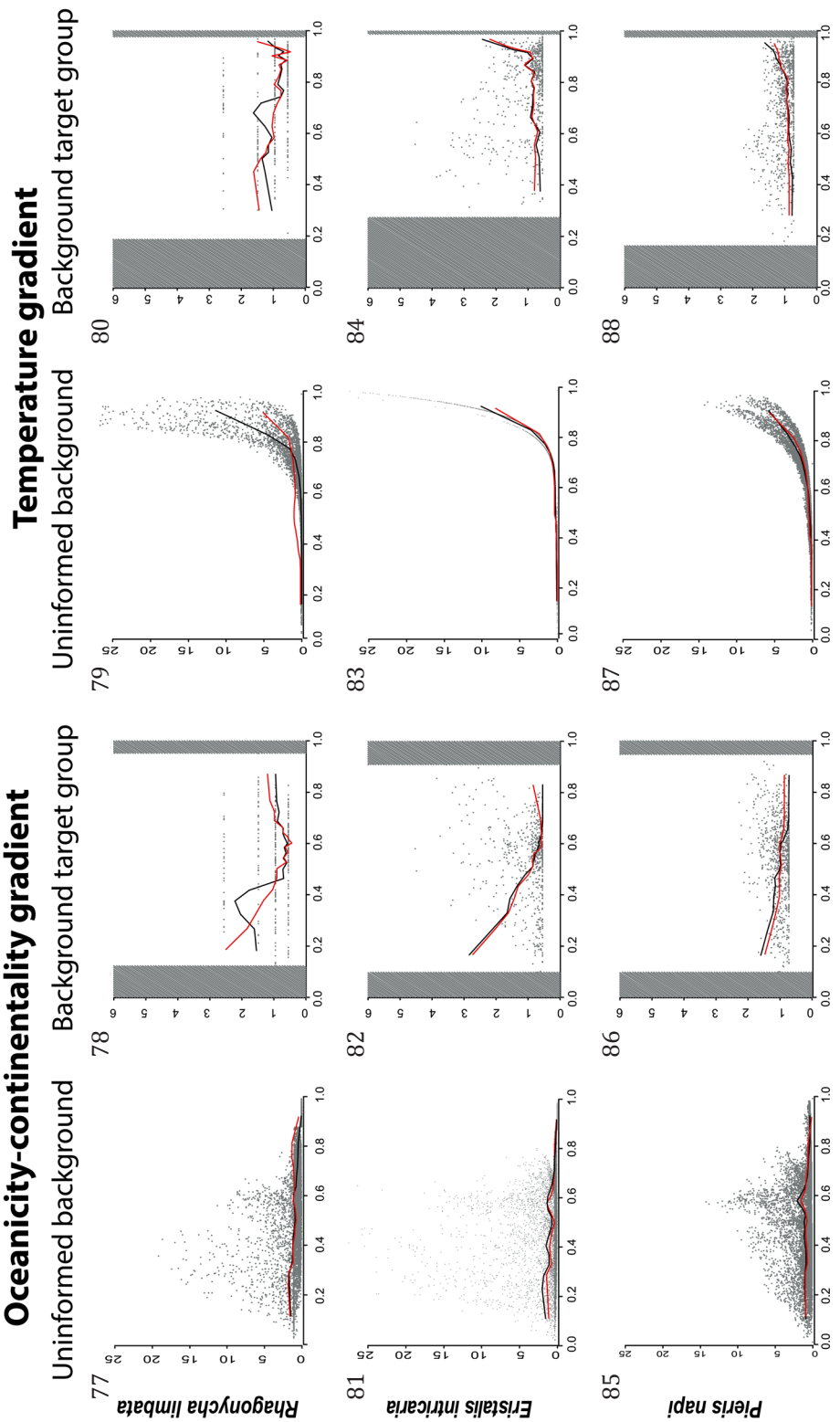
Oceanicity-continentality gradient
Temperature gradient
Uninformed background
Background target group
Uninformed background
Background target group
77
78
79
80
81
82
83
84
85
86
87
88
Rhagonycha limbata
Eristalis intricaria
Pieris napi

RESULTS: COMPARISON BETWEEN MAXENT MODELS

The tests for differences in performance (measured by tAUC) among MaxEnt models obtained with different model selection methods (i.e., the spatial prediction and ecological response models), were non-significant, both for each species and for all nine species together. However, models trained with uninformed background data obtained significantly higher tAUC values than models trained with BTG data (Table 3).

The number of derived variables included in models did not differ significantly among species, but was significantly higher for the spatial prediction models than for the ecological response models, and higher for models trained with uninformed background data than for models trained with BTG data (Table 3).

Table 3. GLM (generalized linear model) tests of the null hypotheses that model type (ecological response model or spatial prediction model), background dataset used (uninformed or BTG), and species identity (nine species) (1) do not affect tAUC (AUC corrected for use with presence-only data) and (2) do not differ with respect to the number of derived variables in MaxEnt models. df = model degrees of freedom (total number of observations = 36). F and p value refer to an F-ratio test of each model against the null model of the intercept only. Trend = category for which the highest value for the response variable was predicted by a model significantly different from the null model.

Response variable	GLM	Predictor	*df*	Deviance explained	F	p value	Trend
tAUC	identity link, normal errors	model type	1	0.034	1.19	0.283	–
		background	1	0.566	44.29	< 0.001	uninformed background
		Species	8	0.260	1.19	0.344	–
No. of derived variables	log link, Poisson errors	model type	1	0.813	168.58	<0.001	spatial prediction model
		background	1	0.529	24.03	<0.001	uninformed background
		Species	8	0.516	1.72	0.089	–

Fig. 89–106: Maps of the geographical distribution of probability-ratio output (PRO) values from the spatial prediction models (SPM) for all nine species, obtained with uninformed background (UB) and background target group (BTG). The scaling of the color gradient differs between maps, except for the value 1 which1, which is always represented by the transition between green- and yellow-colored patches to facilitate comparisons between maps and models. Presence observations are shown as black dots in the uninformed background (UB) maps.

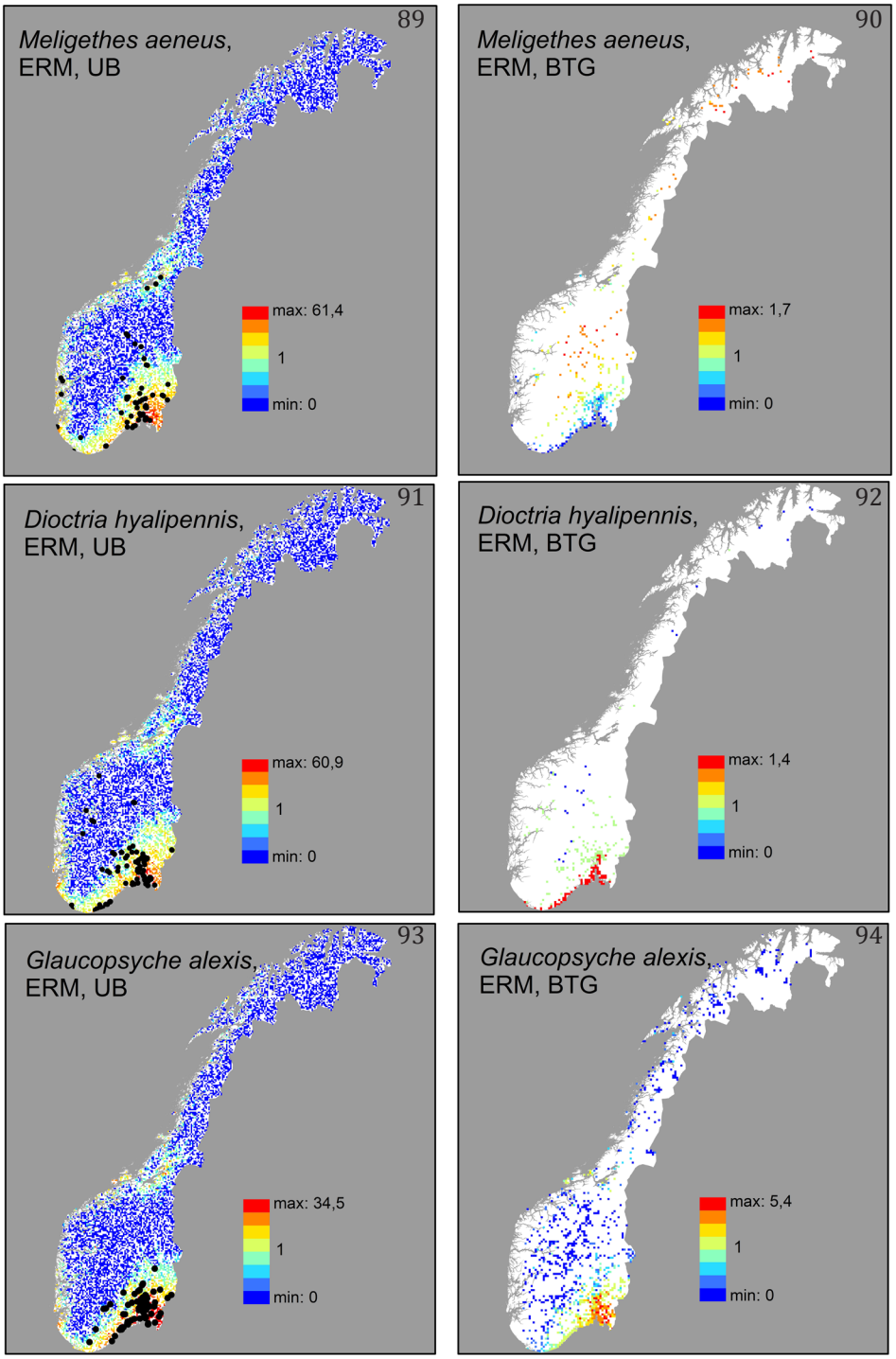
89
Meligethes aeneus,
ERM, UB
max: 61,4
1
min: 0
90
Meligethes aeneus,
ERM, BTG
max: 1,7
1
min: 0
91
Dioctria hyalipennis,
ERM, UB
max: 60,9
1
min: 0
92
Dioctria hyalipennis,
ERM, BTG
max: 1,4
1
min: 0
93
Glaucopsyche alexis,
ERM, UB
max: 34,5
1
min: 0
94
Glaucopsyche alexis,
ERM, BTG
max: 5,4
1
min: 0

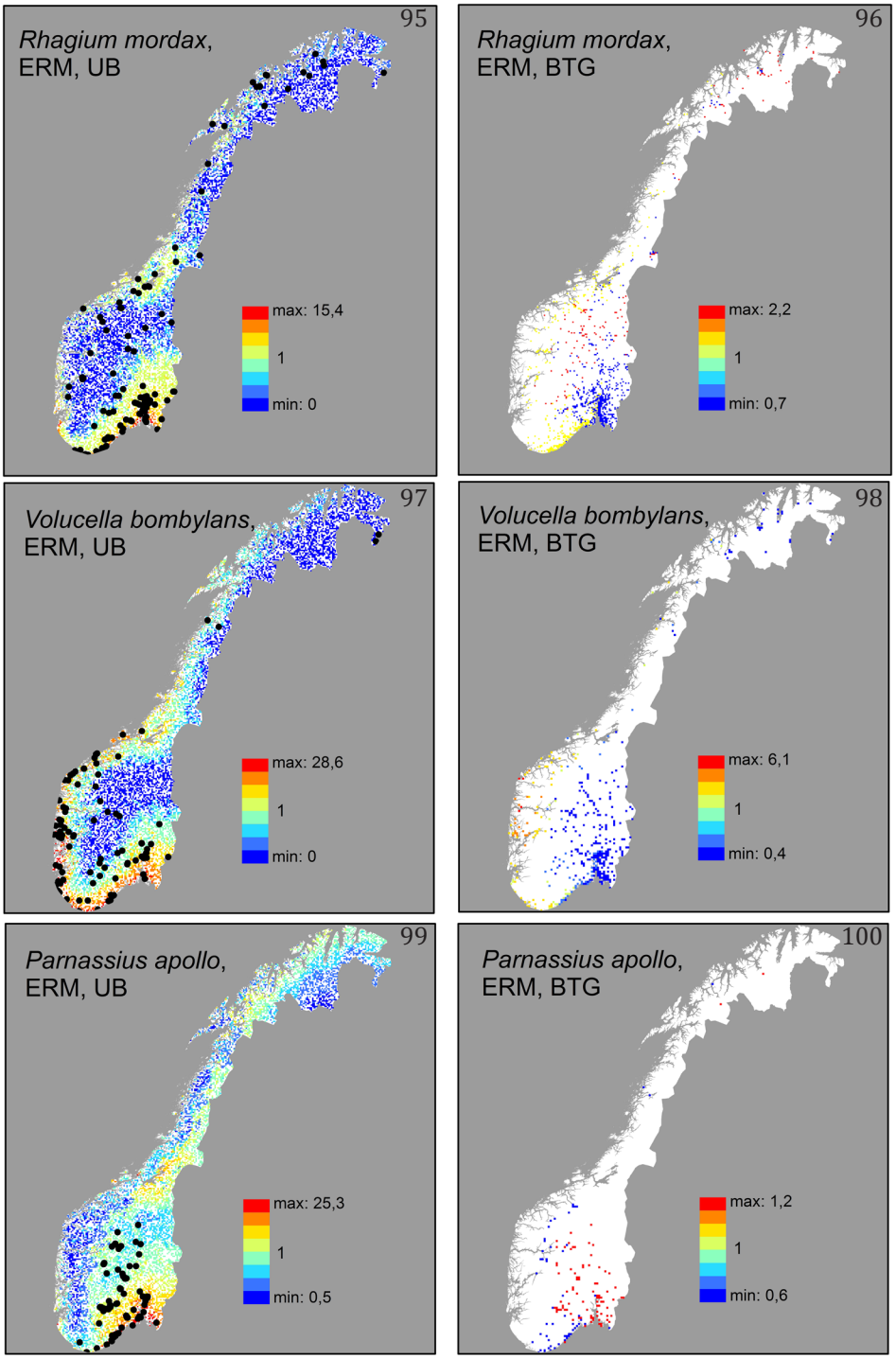
95
Rhagium mordax,
ERM, UB
max: 15,4
1
min: 0
96
Rhagium mordax,
ERM, BTG
max: 2,2
1
min: 0,7
97
Volucella bombylans,
ERM, UB
max: 28,6
1
min: 0
98
Volucella bombylans,
ERM, BTG
max: 6,1
1
min: 0,4
99
Parnassius apollo,
ERM, UB
max: 25,3
1
min: 0,5
100
Parnassius apollo,
ERM, BTG
max: 1,2
1
min: 0,6

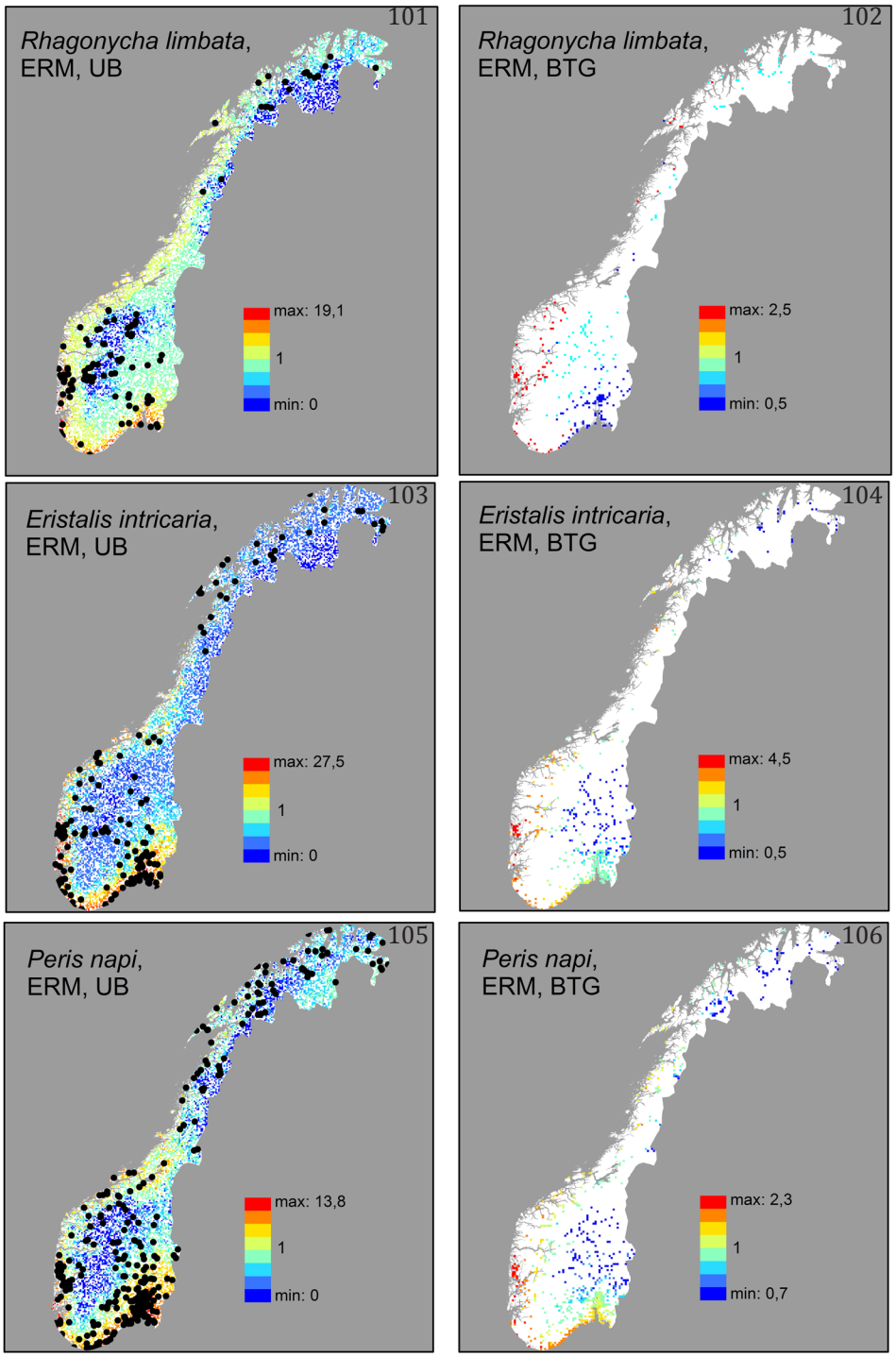
101
Rhagonycha limbata,
ERM, UB
max: 19,1
1
min: 0
102
Rhagonycha limbata,
ERM, BTG
max: 2,5
1
min: 0,5
103
Eristalis intricaria,
ERM, UB
max: 27,5
1
min: 0
104
Eristalis intricaria,
ERM, BTG
max: 4,5
1
min: 0,5
105
Peris napi,
ERM, UB
max: 13,8
1
min: 0
106
Peris napi,
ERM, BTG
max: 2,3
1
min: 0,7

DISCUSSION

DETECTING SAMPLING BIAS

The bias assessment framework relies on two assumptions: (1) that theoretical FoP curves can be used to approximate true FoP curves, with which observed FoP curves can be compared; and consequently, (2) that deviations of observed FoP curves with respect to the major complex-gradients from the expected smooth and unimodal (or truncated unimodal) theoretical FoP curves indicate presence of sampling bias. For all example species, we find larger or smaller discrepancies between observed FoP and theoretical FoP curves. The nature of these discrepancies does not seem to bear any relationship to species-specific properties such as the shape of observed FoP curves or which CURS category. The species belongs to Observed FoP curves along the oceanicity-continentality gradient, calculated with uninformed background data, are more or less distinctly bi- and trimodal and do not resemble ecologically realistic species response curves (cf. Figs 2–9). We therefore interpret these curves as examples of under- and over-sampling of different sections of the gradient. Other deviant curve shapes, such as the weak central mode of the observed FoP curve for *P. napi* (along the oceanicity-continentality gradient and calculated with uninformed background), may either represent a unimodal true response over-sampled near the oceanic extreme and under-sampled for intermediate oceanicity-continentality values, or a monotonously declining response over-sampled near the species' optimum. Access to empirical FoP curves, obtained by use of an independently collected set of presence/absence data (Austin 2007, Edvardsen et al. 2011, Halvorsen 2012), is necessary to decide which of these alternative explanation(s), if any, which actually apply to each case.

The species categorized as satellite, urban and intermediate all show unimodal, although not entirely smooth, observed FoP curves along the oceanicity-continentality gradient when calculated with uninformed background, with irregularities that suggest stochastic variation. Small irregularities in the observed FoP curves are expected if the gradient in question is not the only gradient of importance for the species and, in addition, not fully independent of variation along all other gradients, and/or if the number of presence observations is too small to estimate the observed FoP accurately.

All observed FoP curves along the temperature gradient, calculated with uninformed background, are right truncated, most likely, because all species (with the possible exception of *E. intricaria*) have their optima outside the sampled portion of the gradient (Eliasson et al. 2005, Ehnström & Holmer 2007, Bartsch et al. 2009). Moreover, this observed FoP-curve shape may have been accentuated by over-sampling near the high-temperature extreme of the gradient. The warmest, south-eastern, parts of Norway are the richest in insect host plant species (e.g., Grytnes et al. 1999, Aarvik et al. 2009), have the largest regional insect species pools (Aarvik

Fig. 107–124. Maps of the geographical distribution of probability-ratio output (PRO) values from the ecological response models (ERM) for all nine species, with uninformed background (UB) and background target group (BTG). Background target-group PRO values were only calculated for pixels used as background cells in the modeling. The scaling of the color gradient differs between maps, except for the value 1, which is always represented by the transition between green- and yellow-colored patches to facilitate comparisons between maps and models. Presence observations are shown as black dots in the uninformed background (UB) maps.

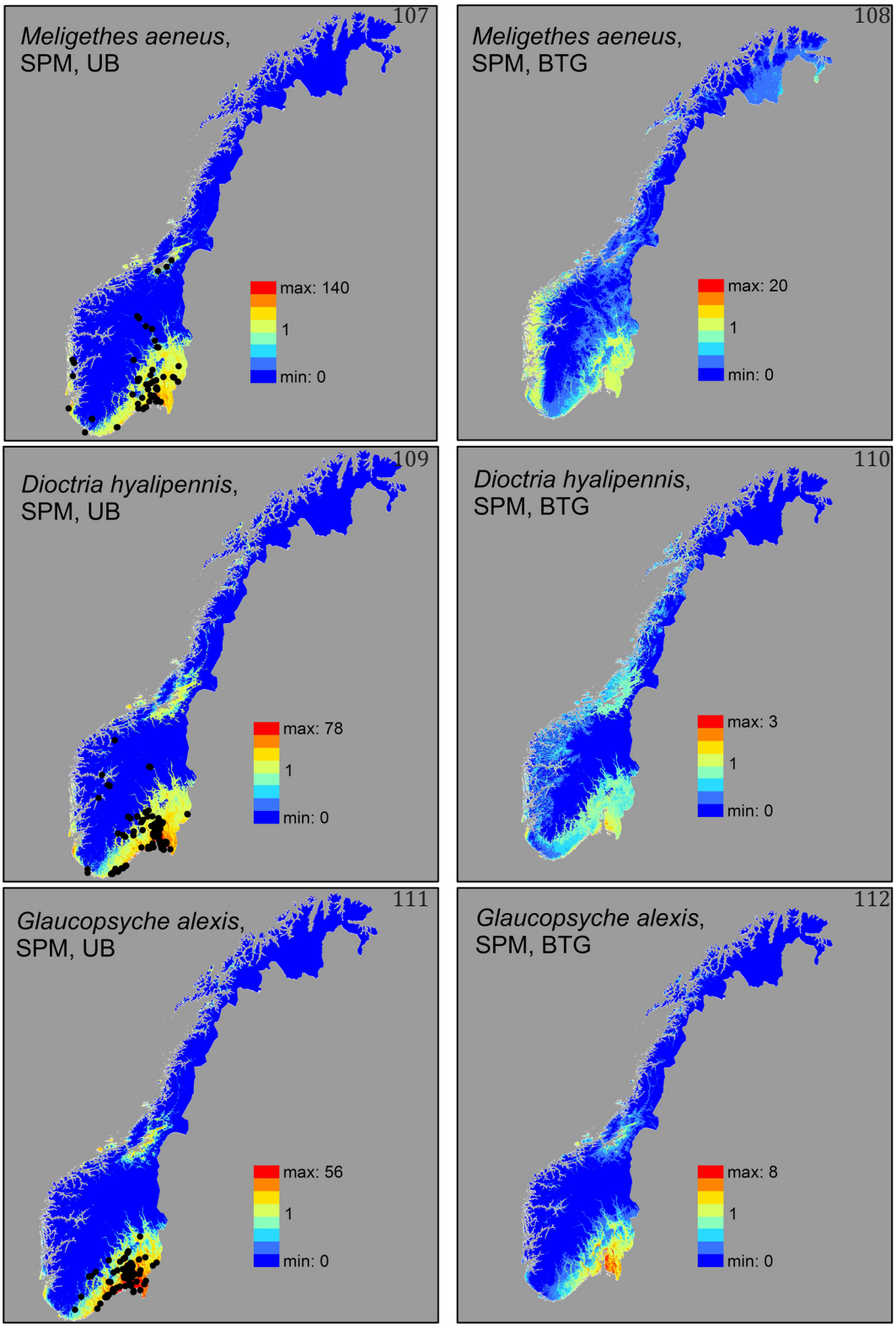
107
Meligethes aeneus,
SPM, UB
max: 140
1
min: 0
108
Meligethes aeneus,
SPM, BTG
max: 20
1
min: 0
109
Dioctria hyalipennis,
SPM, UB
max: 78
1
min: 0
110
Dioctria hyalipennis,
SPM, BTG
max: 3
1
min: 0
111
Glaucopsyche alexis,
SPM, UB
max: 56
1
min: 0
112
Glaucopsyche alexis,
SPM, BTG
max: 8
1
min: 0

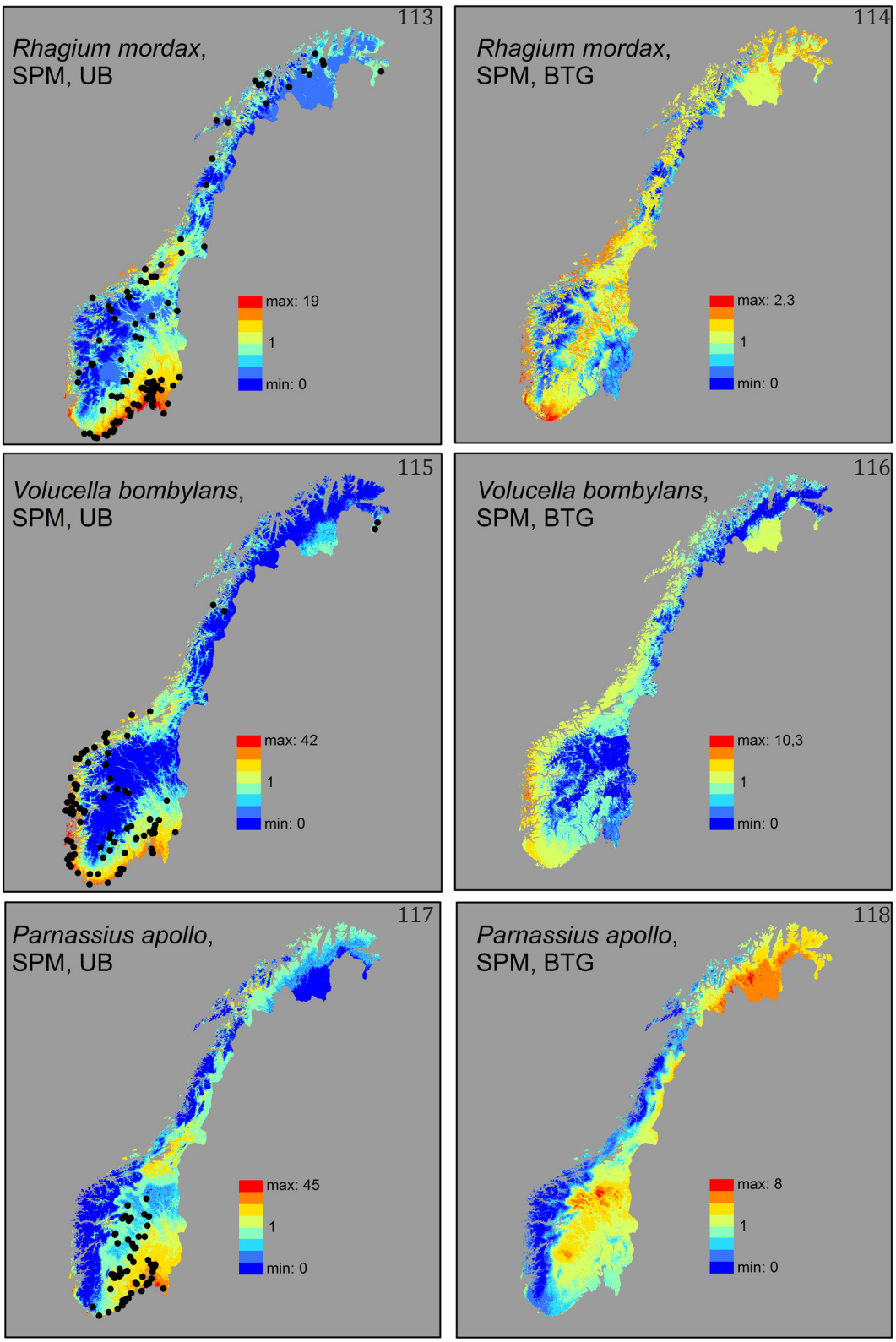
113
Rhagium mordax,
SPM, UB
max: 19
1
min: 0
114
Rhagium mordax,
SPM, BTG
max: 2,3
1
min: 0
115
Volucella bombylans,
SPM, UB
max: 42
1
min: 0
116
Volucella bombylans,
SPM, BTG
max: 10,3
1
min: 0
117
Parnassius apollo,
SPM, UB
max: 45
1
min: 0
118
Parnassius apollo,
SPM, BTG
max: 8
1
min: 0

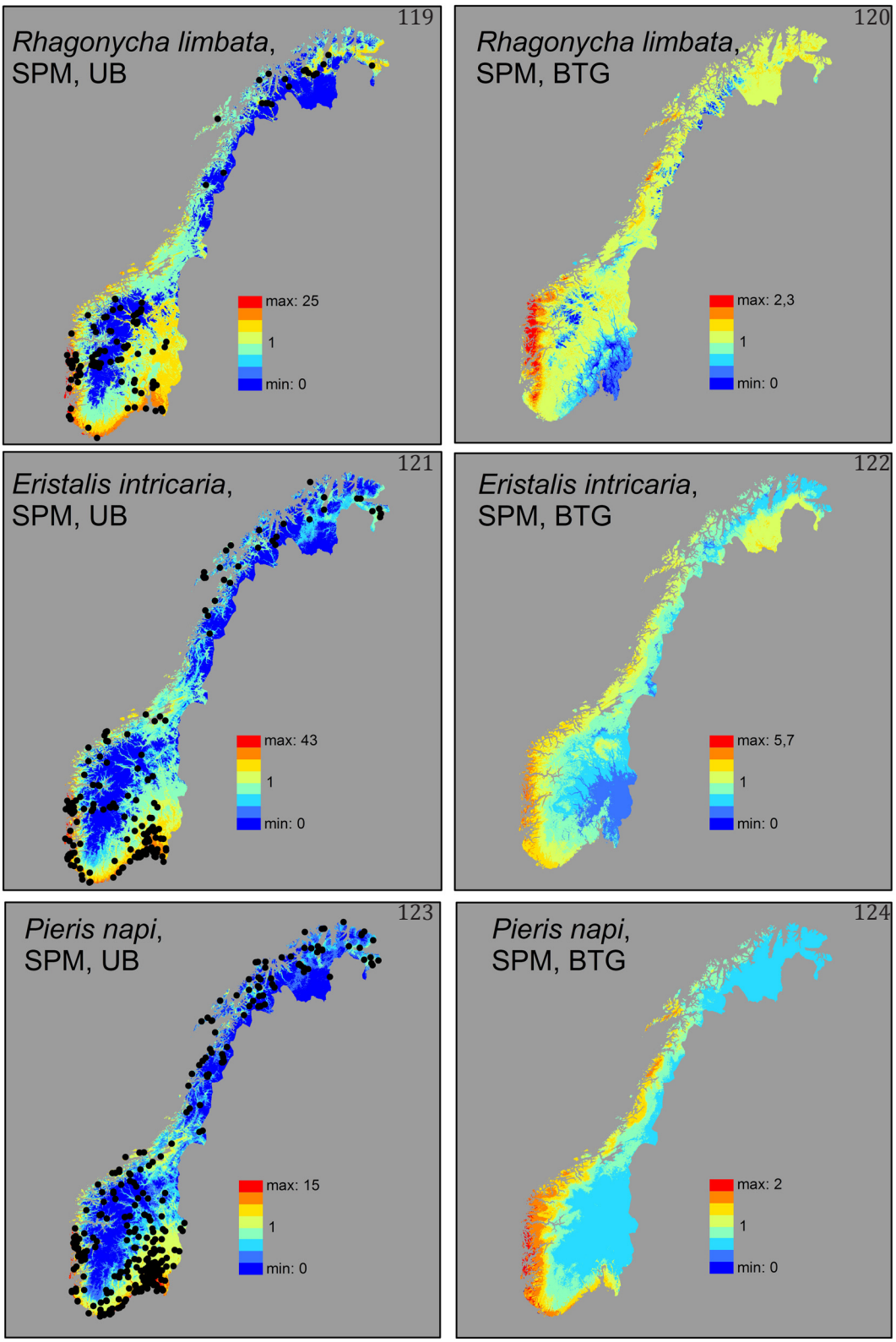
119
Rhagonycha limbata,
SPM, UB
max: 25
1
min: 0
120
Rhagonycha limbata,
SPM, BTG
max: 2,3
1
min: 0
121
Eristalis intricaria,
SPM, UB
max: 43
1
min: 0
122
Eristalis intricaria,
SPM, BTG
max: 5,7
1
min: 0
123
Pieris napi,
SPM, UB
max: 15
1
min: 0
124
Pieris napi,
SPM, BTG
max: 2
1
min: 0

et al. 2009), are most densely populated, and have therefore probably also been subject to the largest insect-collecting effort.

BACKGROUND TARGET GROUP: CORRECTION OF SAMPLING BIAS OR INTRODUCTION OF NEW BIAS?

Contrary to viewpoints expressed in the literature, we find that the observed FoP curves obtained with BTG data deviate more strongly from the expected theoretical FoP curves than the observed FoP curves calculated with uninformed background data. This was most clearly exemplified by *R. limbata*, *P. apollo* and *R. mordax*, for which the shapes of the observed FoP curves change from unimodal (truncated unimodal along the temperature gradient) to complex and almost bimodal, complex and almost monotonous, and a monotonous shape without any trace of unimodality left, respectively, along the two gradients. These results can only be understood by taking properties of the BTG data into account: an observed FoP curve obtained with BTG data is a model for the ratio between the frequency by which the focal species is recorded and the frequency by which the species of the BTG are recorded, as a function of position along a gradient. Thus, by definition, the observed FoP curve obtained with BTG data estimates a quantity different from the targeted species' true FoP with respect to the gradient in question. In fact, flattened observed FoP curves are the logical outcome when the ratio between the probabilities for encountering the focal species and the species of the BTG is more or less constant along the gradient.

The examples also include cases in which sampling bias may have been corrected by BTG: along the oceanicity-continentality gradient, the observed BTG-FoP curve for *E. intricaria* is similar to the corresponding curve calculated with uninformed background, except for being smoother. This indicates a reduction of stochastic sampling bias by BTG. *P. napi* provides another example of possible correction of sampling bias by BTG: whereas the observed uninformed-FoP curve (along the oceanicity-continentality gradient) is bimodal, probably due to oversampling of the left extreme of the gradient and/or under-sampling around 0.4 units along the gradient, the corresponding BTG-curve is increasing more or less rather monotonously.

Observed BTG-FoP curves in this study tend to be more irregular than the corresponding curves calculated with uninformed background. One likely explanation for this is that the BTG datasets are much smaller than the uninformed background datasets (211–1541 observations, compared with more than 10 000, cf. Table 2), which implies that the variance of the observed FoP estimates is higher when calculated from BTG than when calculated from uninformed background data. Sparse data for a realistic background target group, as seen for some of the groups in this study, is likely to be a common situation. Our results thus suggest that great caution is needed when available BTG datasets are small. This agrees with the finding of Phillips & Dudík (2008) that model performance improves with increasing number until ca 10,000 background observations are used. Stokland et al. (2011) do, however, find small effects of varying the number of pseudo-absence observations in species distribution models obtained by boosted regression trees from 64 to over 4000 records compared to effects of sampling design and properties of the focal species. Furthermore, Mateo et al. (2010) claim that species distribution models may be improved by use of BTG datasets consisting of as few as 15 observations. Based upon our results, as well as theoretical reasoning, we however do, seriously, question these claims. Careful studies of the number of observations needed to form a robust BTG dataset, and whether cases exist for which no appropriate BTG dataset can be obtained, are clearly needed.

In contrast to the common view that BTG background is an effective means of mitigating sampling bias in presence-only data (Phillips & Dudík 2008, Phillips et al. 2009, Mateo et al.

2010, Yackulic et al. 2013), we recommend that BTG is used with great caution. BTG background will correct sampling bias in presence-only data if and only if presence observations for the species used for BTG have similar bias as the presence observations of the modelled target and BTG presences cover an interval along each major complex-gradient that extends well beyond the tolerance limits of the focal species. The literature contains many examples of the BTG approach being applied for SDM without data properties being explored prior to modelling and without other background designs being applied in parallel (Graham et al. 2011, Crall et al. 2013). Because results obtained with BTG, that are compared with results obtained with other types of background data, vary from inferior (Heibl & Renner 2012, Millar & Blouin-Demers 2012, Fourcade et al. 2014) to superior (Bystriakova et al. 2012, Kramer-Schadt et al. 2013), we recommend that any use of BTG for SDM should be preceded by careful examination of FoP curves for BTG as well as for other types of background data.

EFFECTS OF SAMPLING BIAS

We show by examples that sampling bias may be disguised in different and, to a large extent, unpredictable ways and that no short cuts exist by which effects of sampling bias on species distribution models can be circumvented. Accordingly, to leave it to the SDM method to 'correct' for sampling bias comes without guarantee and instead incurs a great danger that new bias is introduced. We therefore argue (1) that sampling bias should be judged by the realism of the observed FoP curve as an issue of its own, kept separate from methodological issues related to SDM such as choice of modelling method, and (2) group discriminative SDM methods should be judged by their ability to reproduce observed FoP curves with a degree of detail that matches the level of generalization required by the purpose of the study (Halvorsen 2012).

Predicted relative FoP curves for spatial prediction models as well as ecological response models for the nine example species do, in most cases, resemble the observed FoP curves closely. For the species with the most distinctly unimodal observed FoP curves, the MaxEnt models predict unimodal responses and effectively remove small irregularities in the responses. For the many species with complex and ecologically unrealistic observed FoP, curves, most clearly seen when using the BTG data, predicted relative FoP curves obtained by MaxEnt reflect these patterns. This demonstrates that MaxEnt has the flexibility with respect to the fitted functional relationship required of a good SDM method and explains why MaxEnt often performs best or among the best in comparative tests of SDM methods (e.g., Elith et al. 2006, Mateo et al. 2010, Elith et al. 2011). Furthermore, this shows that data quality is likely to have stronger impact on the quality of SDMs than choice of modelling method.

The number of derived variables in the spatial prediction models is significantly higher than in the ecological response models while the AUC values show no significant difference (Appendix 1–4). Complex models often result when inclusion of many variables of the threshold and hinge types is opened for (Phillips & Dudík 2008, Elith et al. 2011), as is the case with the default spatial prediction models. The spatial prediction model exemplifies complex models for *G. alexis* for uninformed background data. In this model, the oceanicity-continentality variable was represented by nine derived variables, whereas in the corresponding ecological response model this variable was represented by only one variable of the deviation type. Nevertheless, the tAUC values (calculated from the data used to train the model) and the predicted relative FoP curves for the two models are very similar (Fig. 61). This shows that simple models with few parameters (derived variables) can be as good as (and sometimes even better than) more complex models in representing general features of species responses to gradients. Our results

thus concur with previous advice against building overly complex spatial prediction models, which may fail to assist understanding of the focal species' relationship to the environment (Anderson & Gonzalez 2011, Halvorsen 2013, Syfert et al. 2013). Worked examples in this study do, however, also include examples of ecological response models that are too simplistic: in models for *P. apollo* and *D. hyalipennis*, one of the bioclimatic variables was not at all represented by derived variables. The irregular, unimodal shape of the observed FoP curve of the latter clearly indicates that the omitted bioclimatic gradient is of importance for predicting the distribution of the species. In other cases, exemplified by predicted relative FoP curves obtained from BTG data for P. apollo and R. mordax derived variables of the hinge and threshold types give rise to predicted relative FoP curves with long, linear segments along the oceanicity-continentality gradient. These patterns deviate strongly both from the observed and the theoretical FoP curves and demonstrate that these types of derived variables may, and most likely often do, give rise to predicted relative FoP curves with shapes that are ecologically unrealistic. These types of derived variables may therefore be inappropriate for ecological response models, except when responses are truncated, as found in all the nine species with respect to the temperature gradient.

CONCLUSIONS

By applying the suggested bias frameworks on data for nine insect species, we demonstrate that comparison between observed and theoretical FoP curves is a promising tool for detecting and categorizing sampling bias in presence-only data. We show that presence-only data can give rise to observed FoP curves that can deviate strongly from the expected smooth, unimodal or truncated unimodal theoretical FoP curves. Furthermore, we show that these deviations can be confidently interpreted, in most cases, as indications of sampling bias of different types. Strong signs of stochastic variation have been demonstrated for restrictedly distributed species, and large discrepancies between observed and theoretical FoP curves revealed for some of the more widespread species, indicates under- and over-sampling of different portions of influential gradients. We show cases in which the deviation from expected curve shapes remain ambiguous because several mechanisms may explain the observed patterns. However, we also show cases in which the smooth and unimodal observed FoP curves indicate a lack of sampling bias in the data. Furthermore, we show that use of background target group (BTG) data offers no general solution to problems related to sampling bias. We therefore advise against uncritical use of this broadly accepted approach to deal with potential bias in the data and recommend that inspection of observed FoP curves for the focal species, calculated with different kinds of background data, are used to inform the choice of background data for SDM. Our results highlight the importance of disentangling shortcomings of the data from shortcomings of the modelling method, and demonstrate that comparison between observed and predicted relative FoP curves is a potentially important tool in making this distinction. Our study clearly demonstrates that bias in data is more important for the quality of the distribution model than the modelling method as such, supporting similar views axpressed by Lobo (2008). This is important, given the strong focus on choice of method for SDM in recent literature (Elith et al. 2006, Mateo et al. 2010, Fitzpatrick et al. 2013). However, our examples also show the importance of choosing a level of model complexity that is appropriate for the modelling purpose. Spatial prediction models, typically including a significantly higher number of derived variables than ecological response models, do not necessarily perform significantly better than simpler ecological re-

sponse models, even in terms of training AUC. This suggests that simpler models are generally preferable to more complex models, even when models are evaluated by predictive performance in the geographical space.

ACKNOWLEDGEMENTS

We would like to thank Eirik Rindal for valuable help with formatting the figures, Leif Arabic for advices on selection of target species and Anders Endrestøl for extracting data from the insect database at the Natural History Museum in Oslo. We are grateful to Kaare Aagaard (Museum of Natural History and Archaeology, Norwegian University of Science and Technology, Trondheim) and Bjarte Jordal (Bergen Museum, University of Bergen) for proving access to collections and for allowing collection of information on occurrence for selected species. Eli Rinde is thanked for valuable comments on an earlier manuscript version. Finally, we thank Dag Endresen, Oddvar Pedersen and Einar Timdal for help with conversion of geographic coordinates from MGRS to regular UTM format. This study was supported by the Norwegian Research Council MILJØ2015 grant 183318 to Vladimir Gusarov.

REFERENCES

Aarvik, L., Hansen, L.O. & Kononenko, V. 2009. Norges sommerfugler. Håndbok over Norges dagsommerfugler og nattsvermere. – Norwegian Entomological Society & Natural History Museum, Univ. of Oslo, Oslo.

Ahti, T., Hämet-Ahti, L. & Jalas, J. 1968. Vegetation zones and their sections in northwestern Europe. – Annls bot. fenn. 5: 169-211.

Anderson, R.P. 2012. Harnessing the world's biodiversity data: promise and peril in ecological niche modeling of species distributions. – Ann. N.Y. Acad. Sci. 1260: 66-80.

Anderson, R.P. & Gonzalez, I.J. 2011. Species-specific tuning increases robustness to sampling bias in models of species distributions: an implementation with Maxent. – Ecol. Modelling 222: 2796–2811.

Anderson, R.P., Peterson, A.T. & Gómez-Laverde, M. 2002. Using niche-based GIS modeling to test geographic predictions of competitive exclusion and competitive release in South American pocket mice. – Oikos 98: 3–16.

Araújo, M.B. & Guisan, A. 2006. Five (or so) challenges for species distribution modelling. –J. Biogeogr. 33: 1677–1688.

Araújo, M.B. & Luoto, M. 2007. The importance of biotic interactions for modelling species distributions under climate change. – Global Ecol. Biogeogr. 16: 743–753.

Austin, M. 2002. Spatial prediction of species distribution: an interface between ecological theory and statistical modelling. – Ecol. modelling 157: 101–118.

Austin, M. 2007. Species distribution models and ecological theory: a critical assessment and some possible new approaches. – Ecol. Modelling 200: 1–19.

Austin, M. & Smith, T., 1989. A new model for the continuum concept. – Vegetatio 83: 35–47.
Austin, M.P. & Gaywood, M.J., 1994. Current problems of environmental gradients and species response curves in relation to continuum theory. – Journal Veg. Sci. 5: 473–482.
Bakkestuen, V., Erikstad, L. & Halvorsen, R. 2008. Step-less models for regional environmental variation in Norway. – J. Biogeogr. 35: 1906–1922.
Bartsch, H., Binkiewitz, E., Rådén, A. & Nasibov, E. 2009. Nationalnyckeln till Sveriges flora och fauna. Tvåvingar: Blomflugor: Syrphinae. Diptera: Syrphidae: Syrphinae. – ArtDatabanken, Uppsala.
Bean, W.T., Stafford, R. & Brashares, J.S. 2012. The effects of small sample size and sample bias on threshold selection and accuracy assessment of species distribution models. –Ecography 35: 250–258.
Boakes, E.H., McGowan, P.J., Fuller, R.A., Chang-qing, D., Clark, N.E., O'Connor, K. & Mace, G.M. 2010. Distorted views of biodiversity: spatial and temporal bias in species occurrence data. – PLoS ONE 8: 1000385: 1–11.
Boulangeat, I., Gravel, D. & Thuiller, W. 2012. Accounting for dispersal and biotic interactions to disentangle the drivers of species distributions and their abundances. – Ecol. Letters 15: 584–593.
Brown, J.H. 1984. On the relationship between abundance and distribution of species. – Am. Nat. 124: 255–279.
Brown, J.H., Stevens, G.C. & Kaufman, D.M., 1996. The geographic range: size, shape, boundaries, and internal structure. – A. Rev. Ecol. Syst. 27: 597–623.
Bystriakova, N., Peregrym, M., Erkens, R.H., Bezsmertna, O. & Schneider, H. 2012. Sampling bias in geographic and environmental space and its effect on the predictive power of species distribution models. – Syst. Biodiv. 10: 305–315.
Cavanaugh, K.C., Siegel, D.A., Raimondi, P.T. & Alberto, F. 2014. Patch definition in metapopulation analysis: a graph theory approach to solve the mega-patch problem. – Ecology 95: 316-328.
Collins, S.L., Glenn, S.M. & Roberts, D.W., 1993. The hierarchical continuum concept. – J. Veg. Sci. 4: 149–156.
Cox, C.B. & Moore, P.D. 2010. Biogeography: an ecological and evolutionary approach, ed. 8. – Wiley, Chichester.
Crall, A.W., Jarnevich, C.S., Panke, B., Young, N., Renz, M. & Morisette, J. 2013. Using habitat suitability models to target invasive plant species surveys. – Ecol. Appl. 23: 60–72.
Crawley, M.J. 2013. The R book, ed. 2. – Wiley, Chichester.
Dahl, E. & Birks, J., 1998. The phytogeography of Northern Europe. – Cambridge University Press, Cambridge.
Edvardsen, A., Bakkestuen, V. & Halvorsen, R. 2011. A fine-grained spatial prediction model for the red-listed vascular plant *Scorzonera humilis*. – Nord. J. Bot. 29: 495–504.
Ehnström, B. & Holmer, M. 2007. Nationalnyckeln till Sveriges flora och fauna. Skalbaggar: Långhorningar. Coleoptera: Cerambycidae. – ArtDatabanken, Uppsala.
Eliasson, C.U., Ryrholm, N. & Gärdenfors, U. 2005. Nationalnyckeln till Sveriges flora och fauna: Fjärilar. Dagfjärilar: Hesperiidae–Nymphalidae. – ArtDatabanken, Uppsala.
Elith, J., Graham, C.H., Anderson, R.P., Dudik, M., Ferrier, S., Guisan, A., Hijmans, R.J., Huettmann, F., Leathwick, J.R., Lehmann, A., Li, J., Lohmann, L.G., Loiselle, B.A., Manion, G., Moritz, C., Nakamura, M., Nakazawa, Y., Overton, J.M., Peterson, A.T., Phillips, S.J., Richardson, K., Scachetti-Pereira, R., Schapire, R.E., Soberon, J., Williams, S., Wisz, M.S. & Zimmermann, N.E. 2006. Novel methods improve prediction of species' distributions from occurrence data. – Ecography 29: 129–151.
Elith, J., Phillips, S.J., Hastie, T., Dudík, M., Chee, Y.E. & Yates, C.J. 2011. A statistical explanation

of MaxEnt for ecologists. – Divers. Distrib. 17: 43–57.
Ellenberg, H. 1954. Über enige Fortschritte der kausalen Vegetationskunde. – Vegetatio 5-6: 199-211.
Erikstad, L., Bakkestuen, V., Bekkby, T. & Halvorsen, R. 2013. Impact of scale and quality of digital terrain models on predictability of seabed terrain types. – Mar. Geod. 36: 2–21.
Fitzpatrick, M., Gotelli, N. & Ellison, A. 2013. MaxEnt versus MaxLike: empirical comparisons with ant species distributions. – Ecosphere 4: 55: 1–15.
Fourcade, Y., Engler, J.O., Rödder, D. & Secondi, J. 2014. Mapping species distributions with MAXENT using a geographically biased sample of presence data: a performance assessment of methods for correcting sampling bias. – PLoS ONE 9: e97322: 1-18.
Franklin, J. 2009. Mapping species distributions: spatial inference and prediction. – Cambridge University Press, Cambridge.
Gaston, K.J., Blackburn, T.M., Greenwood, J.J.D., Gregory, R.D., Quinn, R.M. & Lawton, J.H. 2000. Abundance–occupancy relationships. – J. Appl. Ecol. 37: 39–59.
Gaston, K.J., Chown, S.L. & Evans, K.L. 2008. Ecogeographical rules: elements of a synthesis. – J. Biogeogr. 35: 483–500.
Gauslaa, Y. 1984. Heat resistance and energy budget in different Scandinavian plants. – Ecography 7: 5–78.
Graham, J., Jarnevich, C., Young, N., Newman, G. & Stohlgren, T. 2011. How will climate change affect the potential distribution of Eurasian tree sparrows *Passer montanus* in North America? – Curr. Zool. 57: 648–654.
Grytnes, J.A., Birks, H.J.B. & Peglar, S.M., 1999. Plant species richness in Fennoscandia: evaluating the relative importance of climate and history. – Nord. J. Bot. 19: 489–503.
Guisan, A. & Zimmermann, N.E. 2000. Predictive habitat distribution models in ecology. – Ecol. Modelling 135: 147–186.
Gutiérrez, D., Fernández, P., Seymour, A.S. & Jordano, D. 2005. Habitat distribution models: are mutualist distributions good predictors of their associates? – Ecol. Appl. 15: 3–18.
Halvorsen, R. 2012. A gradient analytic perspective on distribution modelling. – Sommerfeltia 35: 1–165.
Halvorsen, R. 2013. A maximum likelihood explanation of MaxEnt, and some implications for distribution modelling. – Sommerfeltia 36: 1–132.
Halvorsen, R., Mazzoni, S., Bryn, A. & Bakkestuen, V. 2015. Opportunities for improved distribution modelling practice via a strict maximum likelihood interpretation of MaxEnt. – Ecography 38: 172-183.
Hansen, V. & Larsson, S., 1973. Biller X. Blødvinger, klannere m.m.: Malacodermata, Fossipedes, Marcrodactylia og Brachymera. – Danm. Fauna 44: 41–42.
Hanski, I. 1982. Dynamics of regional distribution: the core and satellite species hypothesis. – Oikos: 210–221.
Hanski, I. 1998. Metapopulation dynamics. – Nature 396: 41–49.
Hanski, I. & Ovaskainen, O. 2000. The metapopulation capacity of a fragmented landscape. – Nature 404: 755–758.
Hanski, I. & Simberloff, D., 1997. The metapopulation approach, its history, conceptual domain, and application to conservation. In: Hanski, I. & Gilpin, M.E. (eds.), Metapopulation biology: ecology, genetics, and evolution, Academic Press, San Diego, pp. 5–26.
Hastie, T., Tibshirani, R. & Friedman, J. 2009. The elements of statistical learning, ed. 2. – Springer, New York.
Hatteland, B.A., Roth, S., Andersen, A., Kaasa, K., Støa, B. & Solhøy, T. 2013. Distribution and spread of the invasive slug *Arion vulgaris* Moquin-Tandon in Norway. – Fauna norv. 32: 13–26.
Hebblewhite, M., Merrill, E. & McDonald, T. 2005. Spatial decomposition of predation risk using

resource selection functions: an example in a wolf–elk predator–prey system. – Oikos 111: 101–111.
Heibl, C. & Renner, S.S. 2012. Distribution models and a dated phylogeny for Chilean *Oxalis* species reveal occupation of new habitats by different lineages, not rapid adaptive radiation. – Syst. Biol. 61: 823–834.
Heikkinen, R.K., Luoto, M., Virkkala, R., Pearson, R.G. & Körber, J.-H. 2007. Biotic interactions improve prediction of boreal bird distributions at macro-scales. – Global Ecol. Biogeogr. 16: 754–763.
Hengeveld, R. & Haeck, J., 1982. The distribution of abundance. I. Measurements. – J. Biogeogr. 9: 303–316.
Huston, M.A. 2002. Introductory essay: critical issues for improving predictions. In: Scott, J.M., Heglund, P.J., Morrison, M.L. Haufler, J.B., Raphael, M.G., Wall, W.A. & Samson, F.B. (eds) Predicting species occurrences: issues of accuracy and scale, Island Press, Washington, DC, pp. 7–21.
Jansen, F. & Oksanen, J. 2013. How to model species responses along ecological gradients–Huisman–Olff–Fresco models revisited. – J. Veg. Sci. 24: 1108–1117.
Jaynes, E.T. 1957a. Information theory and statistical mechanics. – Phys. Rev. 106: 620–630.
Jaynes, E.T. 1957b. Information theory and statistical mechanics 2. – Phys. Rev. 108: 171–190.
Jiménez-Valverde, A., Lobo, J. & Hortal, J. 2008. Not as good as they seem: the importance of concepts in species distribution modelling. – Divers. Distrib. 14: 885-890.
Kadmon, R., Farber, O. & Danin, A. 2003. A systematic analysis of factors affecting the performance of climatic envelope models. – Ecol. Appl. 13: 853–867.
Kramer-Schadt, S., Niedballa, J., Pilgrim, J.D., Schröder, B., Lindenborn, J., Reinfelder, V., Stillfried, M., Heckmann, I., Scharf, A.K., Augeri, D.M., Cheyne, S.M., Hearn, A.J., Ross, J., Macdonald, D.W., Mathai, J., Eaton, J., Marshall, A.J., Semiadi, G., Rustam, R., Bernard, H., Alfred, R., Samejima, H., Duckworth, J.W., Breitenmoser-Wuersten, C., Belant, J.L., Hofer, H. & Wilting, A. 2013. The importance of correcting for sampling bias in MaxEnt species distribution models. – Divers. Distrib. 19: 1366-1379.
Leathwick, J. & Austin, M. 2001. Competitive interactions between tree species in New Zealand's old-growth indigenous forests. – Ecology 82: 2560–2573.
Lobo, J.M. 2008. More complex distribution models or more representative data? – Biodiv. Inform. 5: 14–19.
Loehle, C. 2012. Relative frequency function models for species distribution modeling. – Ecography 35: 487–498.
Loiselle, B.A., Jørgensen, P.M., Consiglio, T., Jiménez, I., Blake, J.G., Lohmann, L.G. & Montiel, O.M. 2008. Predicting species distributions from herbarium collections: does climate bias in collection sampling influence model outcomes? – J. Biogeogr. 35: 105–116.
MacKenzie, D.I., Nichols, J.D., Royle, J.A., Pollock, K.H., Bailey, L.L. & Hines, J.E. 2005. Occupancy estimation and modeling: inferring patterns and dynamics of species occurrence. – Academic Press, Amsterdam.
Mateo, R.G., Croat, T.B., Felicísimo, Á.M. & Muñoz, J. 2010. Profile or group discriminative techniques? Generating reliable species distribution models using pseudo-absences and target-group absences from natural history collections. – Divers. Distrib. 16: 84–94.
Mazzoni, S., Halvorsen, R. & Bakkestuen, V. 2015. MIAT: Modular R-wrappers for flexible implementation of MaxEnt Distribution Modelling. – Ecol. Informatics 30: 215-221.
McGill, B. & Collins, C. 2003. A unified theory for macroecology based on spatial patterns of abundance. – Evol. Ecol. Res. 5: 469–492.
Meier, E.S., Kienast, F., Pearman, P.B., Svenning, J.-C., Thuiller, W., Araújo, M.B., Guisan, A. & Zimmermann, N.E. 2010. Biotic and abiotic variables show little redundancy in explaining

tree species distributions. – Ecography 33: 1038–1048.
Merow, C., Smith, M.J. & Silander, J.A. 2013. A practical guide to MaxEnt for modeling species' distributions: what it does, and why inputs and settings matter. – Ecography 36: 1058–1069.
Millar, C.S. & Blouin-Demers, G. 2012. Habitat suitability modelling for species at risk is sensitive to algorithm and scale: A case study of Blanding's turtle, *Emydoidea blandingii*, in Ontario, Canada. – J. Nat. Conserv. 20: 18–29.
Minchin, P.R. 1989. Montane vegetation of the Mt. Field massif, Tasmania: a test of some hypotheses about properties of community patterns. – Vegetatio 83: 97–110.
Moen, A. 1999. National atlas of Norway: vegetation. – Norwegian Mapping Authority, Hønefoss.
Oksanen, J. & Minchin, P.R. 2002. Continuum theory revisited: what shape are species responses along ecological gradients? – Ecol. Modelling 157: 119–129.
Pearce, J. & Ferrier, S. 2000. Evaluating the predictive performance of habitat models developed using logistic regression. – Ecol. Modelling 133: 225–245.
Pellissier, L., Pradervand, J.-N., Pottier, J., Dubuis, A., Maiorano, L. & Guisan, A. 2012. Climate-based empirical models show biased predictions of butterfly communities along environmental gradients. – Ecography 35: 684–692.
Phillips, S.J., Anderson, R.P., Dudík, M., Schapire, R.E. & Blair, M.E. 2017. Opening the black box: an open-source release of Maxent. – Ecography 40: 887-893.
Phillips, S.J., Anderson, R.P. & Schapire, R.E. 2006. Maximum entropy modeling of species geographic distributions. – Ecol. Modelling 190. 231–259.
Phillips, S.J. & Dudík, M. 2008. Modeling of species distributions with Maxent: new extensions and a comprehensive evaluation. – Ecography 31: 161–175.
Phillips, S.J., Dudík, M., Elith, J., Graham, C.H., Lehmann, A., Leathwich, J.R. & Ferrier, S. 2009. Sample selection bias and presence-only distribution models: implications for background and pseudo-absence data. – Ecol. Appl. 19: 181–197.
Phillips, S.J., Dudík, M. & Schapire, R. 2004. A maximum entropy approach to species distribution modeling. – In: Anonymous (ed.), Proceedings of the 21st international conference on machine learning, ACM Press, New York, pp. 655-662.
Phillips, S.J. & Elith, J. 2010. POC plots: calibrating species distribution models with presence-only data. – Ecology 91,: 2476-2484.
Primack, R.B. & Miao, S.L., 1992. Dispersal can limit local plant distribution. – Conserv. Biol. 6,:513–519.
Redfern, J., Ferguson, M., Becker, E., Hyrenbach, K., Good, C.P., Barlow, J., Kaschner, K., Baumgartner, M.F., Forney, K., Ballance, L. 2006. Techniques for cetacean–habitat modeling. – Mar. Ecol. Prog. Ser. 310: 281-295.
Reineking, B. & Schröder, B. 2006. Constrain to perform: regularization of habitat models. – Ecol. Model. 193: 675–690.
Renner, I.W., & Warton, D.I. 2013. Equivalence of MAXENT and Poisson point process models for species distribution modeling in ecology. – Biometrics 69: 274–281.
Robertson, M.P., Cumming, G.S. & Erasmus, B.F.N. 2010. Getting the most out of atlas data. – Divers. Distrib. 16: 363-375.
Rydgren, K., Økland, R.H. & Økland, T. 2003. Species response curves along environmental gradients: a case study from SE Norwegian swamp forests. – J. Veg. Sci. 14: 869–880.
Schweiger, O., Heikkinen, R.K., Harpke, A., Hickler, T., Klotz, S., Kudrna, O., Kühn, I., Pöyry, J. & Settele, J. 2012. Increasing range mismatching of interacting species under global change is related to their ecological characteristics. – Global Ecol. Biogeogr. 21: 88–99.
Searcy, C.A. & Shaffer, H.B. 2014. Field validation supports novel niche modeling strategies in a

cryptic endangered amphibian. – Ecography 37: 983-992.
Shmida, A. & Wilson, M.V. 1985. Biological determinants of species diversity. – J. Biogeogr. 12: 1-20.
Skre, O. 1979. The regional distribution of vascular plants in Scandinavia with requirements for high summer temperatures. – Nor. J. Bot. 26: 295–318.
Soberon, J. & Peterson, A.T. 2005. Interpretation of models of fundamental ecological niches and species' distributional areas. – Biodivers. Informatics 2: 1-10..
Stokland, J.N., Halvorsen, R. & Støa, B. 2011. Species distribution modelling—Effect of design and sample size of pseudo-absence observations. – Ecol. Model. 222: 1800–1809.
Syfert, M.M., Smith, M.J. & Coomes, D.A. 2013. – PloS one 8: e55158: 1–10.
ter Braak, C.J.F. & Prentice, I.C., 1988. A theory of gradient analysis. – Adv. Ecol. Res. 18: 271–317.
Tibshirani, R. 1996. Regression shrinkage and selection via the lasso. – J. R. Statist. Soc. Ser. B 58: 267-288.
Vollering, J., Mazzoni, S. & Halvorsen, R. 2016. Package 'MIAmaxent' Version 0.3.7. – The R foundation for statistical computing, http://cran.r-project.org.
Warren, D.L. & Seifert, S.N. 2011. Ecological niche modeling in Maxent: the importance of model complexity and the performance of model selection criteria. – Ecol. Appl. 21: 335–342.
Westley, P.A., Ward, E.J. & Fleming, I.A. 2013. Fine-scale local adaptation in an invasive freshwater fish has evolved in contemporary time. – Proc. R. Soc. B: Biol. Sci. 280: e20122327.
Whittaker, R.H. 1956. Vegetation of the Great Smoky Mountains. – Ecol. Monogr. 26: 1–80.
Whittaker, R.H. 1967. Gradient analysis of vegetation. – Biol. Rev. 42: 207–264.
Wollan, A.K., Bakkestuen, V., Kauserud, H., Gulden, G. & Halvorsen, R. 2008. Modelling and predicting fungal distribution patterns using herbarium data. – J. Biogeogr. 35: 2298–2310.
Yackulic, C.B., Chandler, R., Zipkin, E.F., Royle, J.A., Nichols, J.D., Grant, E.H.C. & Veran, S. 2013. Presence-only modelling using MAXENT: when can we trust the inferences? – Meth. Ecol. Evol. 4: 236–243.
Økland, R.H. 1986. Rescaling of ecological gradients. II. The effect of scale on symmetry of species response curves. – Nord. J. Bot. 6: 661–670.
Økland, R.H. 1990. Vegetation ecology: theory, methods and applications with reference to Fennoscandia. – Sommerfeltia Suppl. 1: 1-233.
Økland, R.H. 1992. Studies in SE Fennoscandian mires: relevance to ecological theory. – J. Veg. Sci. 3: 279–284.

Appendix 1. Derived variables and their coefficients in the nine ERM models fitted with uninformed background. Types of derived variables: Dev = deviation, Hrk = reverse hinge, Hfk = forward hinge, Thk = threshold. Threshold variables are supplied with information about the knot, i.e. the position of the breaking-point along the explanatory variable. Hinge variables are also supplied with information about the knot, i.e., the point along the explanatory variable where values change from 0 to nonzero. This information is given as quantile class (1 to 20).

Species	AUC	Environmental variable	Derived variable	Coefficient
Dioctria hyalipennis	0.944	Oceanicity–continentality	Dev1	–3.872
			HRk14	1.061
		Temperature	Dev08	8.312
Eristalis intricaria	0.872	Oceanicity–continentality	HRk08	–0.017
			HRk13	0.327
			HRk18	–2.029
		Temperature	Dev14	3.440
			ZSk	3.490
Glaucopsyche alexis	0.963	Oceanicity–continentality	Dev2	–5.905
		Temperature	HFk18	–15.019
Rhagonycha limbata	0.717	Oceanicity–continentality	HRk09	–0.076
			HRk18	–2.777
		Temperature	Dev16	2.915
			HFk11	–3.656
Meligethes aeneus	0.936	Oceanicity–continentality	Dev1	–3.865
		Temperature	Dev07	8.171
Parnassius apollo	0.853	Oceanicity–continentality	Dev2	–4.102
			HRk09	1.364
		Temperature	Dev10	2.614
			HRk18	0.794
Pieris napi	0.803	Oceanicity–continentality	Dev1	–1.364
			Dev13	1.874
		Temperature	Dev08	4.585
Rhagium mordax	0.849	Oceanicity–continentality	Dev3	–4.127
			HRk14	0.232
		Temperature	Dev05	6.234
Volucella bombylans	0.890	Oceanicity–continentality	Dev05	–0.612
			HRk14	–0.510
		Temperature	Dev07	3.041
			Dev12	3.028

Appendix 2. Derived variables and their coefficients in the nine ERM models fitted with target background. Types of derived variables: Dev = deviation, Hrk = reverse hinge, Hfk = forward hinge, Thk = threshold. Threshold variables are supplied with information about the knot, i.e. the position of the breaking point along the explanatory variable. Hinge variables are also supplied with information about the knot, i.e., the point along the explanatory variable where values change from 0 to nonzero. This information is given as quantile class (1 to 20).

Species	AUC	Environmental variable	Derived variable	Coefficient
Dioctria hyalipennis	0.588	Temperature	Thk10	4.047
			Thk18	0.473
Eristalis intricaria	0.651	Oceanicity–continentality	HRk14	1.741
		Temperature	HFk18	0.893
Glaucopsyche alexis	0.825	Oceanicity–continentality	Dev2	–4.080
			Thk14	0.758
		Temperature	HRk18	–10.780
			ZSk	–2.643
Rhagonycha limbata	0.658	Oceanicity–continentality	Thk08	–1.000
		Temperature	Thk14	–0.550
Meligethes aeneus	0.614	Temperature	Linear	2.090
			Thk09	3.421
Parnassius apollo	0.572	Oceanicity–continentality	Thk10	0.709
Pieris napi	0.570	Oceanicity–continentality	HRk14	0.724
		Temperature	HFk16	0.583
Rhagium mordax	0.588	Oceanicity–continentality	Thk10	–0.563
		Temperature	Thk10	–0.586
Volucella bombylans	0.718	Oceanicity–continentality	HRk13	1.566
			Thk10	–1.090

Appendix 3. Derived variables and their coefficients in the nine SPM models fitted with uninformed background. Types of derived variables: Dev = deviation, Hrk = reverse hinge, Hfk = forward hinge, Thk = threshold. Threshold variables are supplied with information about the knot, i.e. the position of the breaking point along the explanatory variable. Hinge variables are also supplied with information about the knot, i.e., the point along the explanatory variable where values change from 0 to nonzero. The oceanicity–continentality gradient spans the interval from –0.00493 to 0.00438 and the temperature gradient spans the interval from –0.0056 to 0.00477.

Species	AUC	Environmental variable	Derived variable	Coefficient
Dioctria hyalipennis	0.957	Oceanicity–continentality	Quadratic	–2.360
			Thk –0.00116	0.012
			Thk –0.00106	0.199
			Thk –0.00042	0.063
			Thk 0.00221	0.367
			Thk 0.00250	1.448
			HRk –0.00020	–2.635
			Thk 0.00047	–0.175
			Thk 0.00085	–0.116
			Thk 0.00053	–0.007
		Temperature	Linear	8.793
			Quadratic	1.143
			Thk 0.00093	1.854
			Thk 0.00363	0.036
			Thk 0.00366	0.367
			HFk 0.00308	0.082
			Thk 0.00435	–0.434
			Thk 0.00115	–0.519
			HFk 0.00420	–0.099
			HFk 0.00343	0.085
			Thk 0.00210	–0.121
			Thk 0.00164	–0.049
			HFk 0.00341	0.078
			HFk 0.00335	0.048
		Interaction	Interaction	3.235
Eristalis intricaria	0.883	Oceanicity–continentality	Linear	2.976
			Quadratic	–0.034
			Thk –0.00005	0.153
			Thk –0.00008	0.212
			Thk –0.00296	–0.483
			Thk 0.00237	0.306
			Hfk 0.00296	–2.779
			Thk –0.00020	0.059
			Thk –0.00040	0.006
			Thk 0.00039	–0.205
			Thk 0.00070	–0.023
			Thk 0.00095	–0.016
			Thk 0.00073	–0.001

Appendix 3 (Continued).

Species	AUC	Environmental variable	Derived variable	Coefficient
		Temperature	Linear	1.403
			Quadratic	4.546
			Thk –0.00053	0.454
			HRk –0.00019	–4.436
			Thk 0.00433	–0.357
			HRk –0.00017	–1.145
			Hfk 0.00463	0.032
		Interaction	Interaction	–2.113
Glaucopsyche alexis	0.97	Oceanicity–continentality	Linear	0.807
			Quadratic	–6.245
			Thk –0.00110	0.579
			Thk –0.00076	0.094
			Thk –0.00039	0.168
			Thk –0.00029	0.253
			Thk 0.00064	0.032
			Thk 0.00029	–0.163
			Thk 0.00007	–0.057
		Temperature	Linear	16.089
			HFk 0.00386	–0.025
			HFk 0.00385	–1.719
			Hfk 0.00375	–0.315
		Interaction	Interaction	4.652
Rhagonycha limbata	0.76	Oceanicity–continentality	Linear	2.593
			Quadratic	1.407
			Thk 0.00282	–0.709
			HFk 0.00282	–3.326
			Thk –0.00110	–0.199
			Thk –0.00371	0.046
			HRk –0.00372	–0.374
			HRk –0.00337	–0.146
			HRk –0.00370	–0.305
			Hfk 0.00280	–0.233
		Temperature	Quadratic	2.087
			Thk 0.00331	0.200
			Thk –0.00178	0.973
			Hfk 0.00301	0.149
			Hfk 0.00302	0.084
			Thk 0.00049	–0.141
			HRk –0.0035	–2.099
			Hfk 0.00302	0.092
			HFk 0.00304	0.077
			Hfk 0.00305	0.282
			Hfk 0.003056	0.080
			HRk –0.0026	–0.735
			Hfk 0.00306	0.061

Appendix 3 (Continued).

Species	AUC	Environmental variable	Derived variable	Coefficient
			HRk –0.00025	–0.242
			HRk –0.00004	–1.246
		Interaction	Interaction	–1.522
Meligethes aeneus	0.95	Oceanicity–continentality	Linear	8.035
			Quadratic	–1.497
			HFk 0.00081	–0.594
			HFk 0.00080	–0.258
		Temperature	Linear	12.490
			Hfk 0.00323	0.212
			Hfk 0.00443	1.229
			Hfk 0.00329	0.218
			Hfk 0.00331	0.094
Parnassius apollo	0.879	Oceanicity–continentality	Quadratic	–6.093
			Thk –0.00085	0.448
			Thk 0.00116	–0.091
			Thk –0.00023	0.228
			Thk 0.00050	–0.181
			Thk –0.00020	0.282
			Thk 0.00035	–0.192
			Thk 0.00241	0.697
			Thk 0.00216	0.339
			HRk –0.00015	–0.296
			HRk –0.00014	–0.733
			HRk –0.00010	–1.382
			HRk –0.00009	–0.397
			Thk 0.00041	–0.003
		Temperature	Linear	1.693
			Quadratic	1.033
			Thk 0.00077	0.512
			Thk0.00005	0.668
			Hfk 0.00347	0.015
			Hfk 0.00323	0.450
			Hfk 0.00322	0.426
			Hfk 0.00322	0.733
			Hfk 0.00432	–0.350
			Thk 0.00194	–0.256
Pieris napi	0.813	Oceanicity–continentality	Linear	1.416
			Thk–0.00095	0.312
			Thk –0.00034	0.186
			Thk 0.00305	–1.163
			Thk 0.00049	0.081
			Thk 0.00232	0.204
			Thk –0.00302	–0.243
			Thk –0.00182	0.053
			HRk –0.00395	–0.221

Appendix 3 (Continued).

Species	AUC	Environmental variable	Derived variable	Coefficient
			Hfk 0.00305	–0.642
			Thk 0.00270	–0.069
			Hfk 0.00304	–0.197
			Hfk 0.00293	–0.086
		Temperature	Linear	3.538
			Quadratic	1.823
			Thk 0.00313	0.173
			Thk –0.00113	0.503
			Thk –0.00241	0.071
			Hfk 0.00307	0.028
			Thk 0.00437	–0.405
			HRk 0.00031	–0.949
			Thk 0.00331	0.020
			Hfk 0.00302	0.010
		Interaction	Interaction	–0.921
Rhagium mordax	0.87	Oceanicity–continentality	Linear	2.212
			Quadratic	–3.676
			Thk 0.00225	0.866
			Thk 0.00121	0.186
			Thk 0.00189	0.338
			Hfk 0.00162	0.600
			Hfk 0.00162	0.681
			Hfk 0.00160	0.310
		Temperature	Linear	5.630
			Quadratic	1.337
			Thk –0.00055	0.495
			Thk –0.00110	1.372
			Hfk 0.00422	–3.472
			Thk 0.00031	–0.159
		Interaction	Interaction	–2.203
Volucella bombylans	0.904	Oceanicity–continentality	Linear	3.741
			Quadratic	1.686
			Thk 0.00127	–1.382
			Thk 0.00066	0.093
			Thk –0.00393	0.109
		Temperature	Linear	7.185
			Quadratic	1.349
			Thk –0.00046	0.587
			Thk 0.00419	0.012
			Thk 0.00443	–0.330
			Linear	–0.141
			Thk 0.00127	–0.026
			Hfk 0.00378	0.031
		Interaction	Interaction	–2.688

Appendix 4. Derived variables and their coefficients in the nine SPM models fitted with target background. Types of derived variables: Dev = deviation, Hrk = reverse hinge, Hfk = forward hinge, Thk = threshold. Threshold variables are supplied with information about the knot, i.e. the position of the breaking point along the explanatory variable. Hinge variables are also supplied with information about the knot, i.e., the point along the explanatory variable where values change from 0 to nonzero. The oceanicity–continentality gradient spans the interval from –0.00493 to 0.00438 and the temperature gradient spans the interval from –0.0056 to 0.00477.

Species	AUC	Environmental variable	Derived variable	Coefficient
Dioctria hyalipennis	0.648	Oceanicity–continentality	Linear	–0.569
			Thk 0.00086	–0.203
			Thk 0.00054	–0.097
		Temperature	Quadratic	0.401
			Thk 0.00090	1.137
			Hfk 0.00353	0.414
			Hfk 0.00440	0.200
			Hfk 0.00353	0.157
			Thk 0.00218	–0.182
			Hfk 0.00341	0.102
			Thk 0.00147	–0.048
			Thk 0.00132	–0.031
		Interaction	Interaction	1.650
Eristalis intricaria	0.674	Oceanicity–continentality	Quadratic	0.315
			Thk –0.00073	–0.161
			Thk –0.00153	–0.065
			Thk 0.00039	–0.195
			Thk 0.00236	0.229
			Thk 0.00048	–0.064
		Temperature	Thk 0.00411	0.154
			Hfk 0.00369	0.276
			Hfk 0.00464	–11.424
			Hfk 0.00430	0.330
		Interaction	Interaction	–1.160
Glaucopsyche alexis	0.835	Oceanicity–continentality	Quadratic	–3.161
			Thk –0.00110	0.076
		Temperature	Linear	7.459
			Thk 0.00167	0.198
			Thk 0.00399	–0.015
			Hfk 0.00374	–0.665
			Hfk 0.00372	–1.030
		Interaction	Interaction	4.162
Rhagonycha limbata	0.678	Oceanicity–continentality	Linear	–0.861
			Quadratic	0.240
			Thk –0.00101	–0.024
			Hfk 0.00280	–0.444
		Temperature	Linear	–2.231
			Hfk 0.00400	0.215
			Hfk 0.00399	0.307

Appendix 4 (Continued).

Species	AUC	Environmental variable	Derived variable	Coefficient
			HRk –0.00128	–1.966
			HRk –0.00152	–0.327
			Hfk 0.00307	0.064
			HRk –0.00074	–0.027
		Interaction	Interaction	–1.783
Meligethes aeneus	0.668	Oceanicity–continentality	Linear	2.504
			Quadratic	0.165
			HRk –0.00227	1.816
		Temperature	Linear	2.716
			Hfk 0.00407	0.218
			HRk 0.00184	–0.909
			Hfk 0.00406	0.681
			Hfk 0.00442	0.855
Parnassius apollo	0.637	Oceanicity–continentality	Linear	1.468
			Quadratic	–0.774
			Thk –0.00023	0.031
			HRk –0.00009	–0.093
			HRk –0.00007	–0.594
			HRk –0.00054	–0.172
			HRk –0.00004	–0.232
			Hfk 0.00247	0.282
		Temperature	Linear	–0.681
			Quadratic	–0.130
			Hfk 0.00419	0.464
			Hfk 0.00431	0.115
		Interaction	Interaction	–1.842
Pieris napi	0.576	Oceanicity–continentality	Thk –0.00162	–0.114
			Thk –0.00016	–0.039
			Thk –0.00244	–0.032
			HRk –0.00130	0.297
		Temperature	Thk 0.00313	0.205
			Hfk 0.00452	0.250
			Hfk 0.00452	–5.877
Rhagium mordax	0.61	Oceanicity–continentality	Linear	–0.119
			Quadratic	–0.402
			Thk –0.00226	0.500
		Temperature	Linear	–0.651
			Thk 0.00031	–0.060
			Thk 0.00358	–0.071
			Thk –0.00110	0.415
			HRk –0.00109	–0.732
			Thk 0.00012	–0.001
			Hfk 0.00422	–0.037
		Interaction	Interaction	–1.979

Appendix 4 (Continued).

Species	AUC	Environmental variable	Derived variable	Coefficient
Volucella bombylans	0.768	Oceanicity–continentality	Quadratic	0.373
			Thk –0.00073	–0.435
			Thk 0.00127p	–0.979
			Hfk 0.00274	0.312
			Hfk 0.00265	1.168
			HRk–0.00383	–0.226
			Thk 0.00067	0.086
		Temperature	Quadratic	–0.306
			Hfk 0.00401	0.526
			Hfk 0.00445	–0.233
			HRk 0.00086	–0.481
			Thk 0.000834	0.044
			Hfk 0.00406	0.008
		Interaction	Interaction	–2.847